

ISSN 2738-2656



**JOURNAL OF ARCHITECTURAL
AND ENGINEERING RESEARCH**

Editor in Chief: Mkhitarian Souren (Republic of Armenia), Doctor of science (mathematics), National University of Architecture and Construction of Armenia

Executive Secretary: Kanetsyan Eghine (Republic of Armenia), Doctor of Philosophy (Ph.D.) in Mathematics, National University of Architecture and Construction of Armenia

Editorial Board:

Vardanyan Yeghiazar (Republic of Armenia), Doctor of Science (Engineering), National University of Architecture and Construction of Armenia

Drozdova Irina (Russian Federation), Doctor of science (Economics), St. Petersburg State University of Architecture and Civil Engineering

Tamrazyan Ashot (Russian Federation), Doctor of Science (Engineering), National Research Moscow State University of Civil Engineering (NRU MGSU)

Danilina Nina (Russian Federation), Doctor of Science (Engineering), National Research Moscow State University of Civil Engineering (NRU MGSU)

Klochko Hasmik (Russian Federation), Doctor of Philosophy (Ph.D.) in Architecture, National Research Moscow State University of Civil Engineering (NRU MGSU)

Gurgenidze David (Georgia), Doctor of Philosophy (Ph.D.) in Technical Sciences, Georgian Technical University

Salukvadze Giorgi (Georgia), Georgian Technical University

Jaroslawn Rajczyk (Poland), Doctor of Science (Engineering), Czestochowa University of Technology
Ulewicz Malgorzata (Poland), Dr. Hab., Czestochowa University of Technology

Donabedian Patrick (France), Doctor of Philosophy (Ph.D.) in Architecture, Laboratory of Medieval and Modern Mediterranean Archeology

Gyulzadyan Hakob (Republic of Armenia), Doctor of Philosophy (Ph.D.) in Engineering, National University of Architecture and Construction of Armenia

Harutyunyan Emma (Republic of Armenia), Doctor of Philosophy (Ph.D.) in Architecture, National University of Architecture and Construction of Armenia

Kertmenjian David (Republic of Armenia), Doctor of science (architecture), National University of Architecture and Construction of Armenia

Markosyan Mher (Republic of Armenia), Doctor of Science (Engineering), National University of Architecture and Construction of Armenia

Aloyan Artyom (Republic of Armenia), Doctor of Philosophy (Ph.D.) in Architecture, National University of Architecture and Construction of Armenia

Dadayan Tigran (Republic of Armenia), Doctor of science (Engineering), National University of Architecture and Construction of Armenia

Gasparyan Marietta (Republic of Armenia), Doctor of science (architecture), National University of Architecture and Construction of Armenia

Deputy Editor-in-Chief: Levonyan Levon (Republic of Armenia), Doctor of Philosophy (Ph.D.) in Engineering, National University of Architecture and Construction of Armenia

Rybnov Yevgeniy (Russian Federation), Doctor of science (Economics), St. Petersburg State University of Architecture and Civil Engineering

Lugovskaya Irina (Russian Federation), Doctor of science (pedagogical science), St. Petersburg State University of Architecture and Civil Engineering

Ter-Martirosyan Armen (Russian Federation), Doctor of Science (Engineering), National Research Moscow State University of Civil Engineering (NRU MGSU)

Semyonov Vyacheslav (Russian Federation), Doctor of Philosophy (Ph.D.) in Engineering, National Research Moscow State University of Civil Engineering (NRU MGSU)

Bryanskaya Yulia (Russian Federation), Doctor of Science (Engineering), National Research Moscow State University of Civil Engineering (NRU MGSU)

Imnadze Nino (Georgia), Doctor of Philosophy (Ph.D.) in Architecture, Georgian Technical University

Kipiani Gela (Georgia), Doctor of science (Engineering), Georgian Technical University

Major Maciej (Poland), Dr. Hab. inż. (engineering), Czestochowa University of Technology

Major Izabela (Poland), Dr. Hab. Eng., Czestochowa University of Technology

Yedoyan Vardges (Republic of Armenia), Doctor of Philosophy (Ph.D.) in Mathematics, National University of Architecture and Construction of Armenia

Stakyan Mihran (Republic of Armenia), Doctor of Science (Engineering), National University of Architecture and Construction of Armenia

Azatyany Karen (Republic of Armenia), Doctor of science (architecture), National University of Architecture and Construction of Armenia

Sarukhanyan Arestak (Republic of Armenia), Doctor of Science (Engineering), National University of Architecture and Construction of Armenia

Shahinyan Samvel (Republic of Armenia), Doctor of science (architecture), National University of Architecture and Construction of Armenia

Rashidyants Karen (Republic of Armenia), Doctor of Philosophy (Ph.D.) in Engineering, National University of Architecture and Construction of Armenia

Khachian Eduard (Republic of Armenia), Doctor of science (Engineering), National University of Architecture and Construction of Armenia

Mamyan Zaruhi (Republic of Armenia), Doctor of Philosophy (Ph.D.) in Architecture, National University of Architecture and Construction of Armenia

The journal is approved for publication by National University of Architecture and Construction of Armenia Scientific and Technical Council

**THE MINISTRY OF EDUCATION, SCIENCE, CULTURE AND SPORTS OF THE
REPUBLIC OF ARMENIA**

**JOURNAL OF ARCHITECTURAL AND
ENGINEERING RESEARCH**

1 (1) 2021



**NATIONAL UNIVERSITY OF ARCHITECTURE AND
CONSTRUCTION OF ARMENIA**

YEREVAN 2021

CONTENT

<i>Avetik Artavazd Arzumanyan</i> <i>Vardan Grigor Tadevosyan</i> <i>Nelli Gagik Muradyan</i> <i>Hovhannes Vachagan Navasardyan</i>	Study of "Saralsk" Deposit for Practical Applications in Construction	3
<i>Maria Martin Badalyan</i> <i>Amalya Karapet Karapetyan</i> <i>Nelli Gagik Muradyan</i> <i>Sona Sahak Ratevosyan</i>	Possibility of Tuff Waste Application in the Production of Thermal Insulation Materials	7
<i>Valeriy Peter Bondarenko</i>	Formation of Stiffness Matrices of Plane Elements Based on High-Order Degree Polynomials	13
<i>Victor Dmitriy Eryomin</i>	On Natural Oscillations of a Thin Elastic Wavy Shell of an Open Profile	18
<i>Yeghisabet Hakob Hayrapetyan</i> <i>Stepan Karen Petrosyan</i>	Construction Features of the High-Precision Laser Rangefinder Light Modulator	26
<i>Marine Ashot Kalantaryan</i> <i>Avetik Artavazd Arzumanyan</i>	Water Absorption Capacity of Irind Mine Pumice	32
<i>Khachik Arthur Shahbazyan</i>	Study of Methods for Assessing the Level of Energy Security and the Ways to Improve	36
<i>Varuzhan Levon Shamyanyan</i>	Use of Various Thin-Layer Settling Schemes for Industrial Wastewater Treatment	43
Requirements for Formulating Scientific Articles and the Supporting Documents		50

UDC 691.213.4

DOI: 10.54338/27382656-2021.1-1

Avetik Artavazd Arzumanyan ^{1*}, Vardan Grigor Tadevosyan ²,Nelli Gagik Muradyan ¹, Hovhannes Vachagan Navasardyan ²¹ National University of Architecture and Construction of Armenia, Yerevan, RA² Horizon 95 Research Laboratory, Yerevan, RA

STUDY OF "SARALSK" DEPOSIT FOR PRACTICAL APPLICATIONS IN CONSTRUCTION

In article the results of research of structural features and technical properties of andesite - basalt stone rock of the "Saralsk" deposit are given. The material is estimated by its mineral - petrographic composition, and the cuts/refinements of stone materials have been made for the microscopic study of mineral-petrographic composition. Researches are conducted according to requirements of acting standards and as a result, it became clear, that the rock consists basically of minerals opacitized hornblende and plagioclase, it doesn't contain any no secondary minerals such as hydroxides of iron, chlorites, epidote, quartz, saricite, etc. Petrographic researches have allowed to determine the species of stone rock. The density, strength, water resistance and frost resistance of stone rock are studied. The suitability of the material for practical application in construction, including for external works, is revealed.

Keywords: structure, texture, density, strength, water resistance, frost resistance.

Introduction

The main features by which a natural stone species can be determined are, as is known, position, structure, mineral and chemical compositions. The Geological phenomena to which rocks owe their origin define: being in nature; position and its association with other rocks; mineral and chemical compositions; structure and texture of the material [1].

The article contains the results of petrographic and technological research of stone rock of the "Saralsk" deposit. Preliminary the material is visually defined as a rock belonging to andesite - basalts. The differentiation of basalts and andesites is the important problem of systematizing igneous rock, as both these groups of rocks are closely connected by continuous transitions between themselves. The difficulty of defining the boundaries between them is that it is difficult to determine the exact quantitative mineral composition. As, they contain an uncrystallized base mass of glass and its devitrification or decomposition products, which makes it absolutely impossible to accurately define the composition under a microscope. Therefore at establishing boundaries the chemical analysis of rock is necessary.

For successful application of natural stone, as an architectural-construction product especially in external works, experimental study of its main qualitative indicators is necessary, among which, research aimed at detection of resistance of material to various external influences is most significant.

Materials and methods

The stone rock of the "Saralsk" deposit for the purpose of establishment of suitability of the material for external application in the form of architectural-construction products is investigated.

According to the technical requirements of the relevant standards, the material is estimated by its mineral - petrographic composition, and also resistance to environmental influence, mainly water and frost resistance. For microscopic study of mineral-petrographic composition, sections of stone material have been made; based on analysis of powder from crushed rock, chemical composition of stone is revealed; density, strength, water and frost resistance are studied on samples-cubes with a rib size of 100 mm.

Researches are spent according to requirements of operating standards [2].

Literary review

The questions of geological-tectonic, petroleum-chemical and geochemical features of the magmatism of the tectonic zone of the Alevrdy ore area of Armenia, where the "Saralsk" deposit is located, are dealt with by numerous researches, on which quaternary emissions of pyroclastic material have a type of areal or multi-outlet eruptions. On relatively strong areas of earth crust of the Debed's rock sets arose faults from which the basalt lava streamed. Numerous crossed cracks were weak places, especially in crossing places where the message with the magmatic pocket was established, and arose craters of volcanoes. Craters of volcanoes existed short time. After eruption the fault cicatrised, at further revival of volcanic activity on the same crack or in new crossing of cracks there was a new center of propagation of basalt lavas, in some cases changing during volcanic history its composition. Basalt and andesite lavas of this region of Armenia, streaming on the surface of the earth and cooling in the form of streams and covers, mainly formed a blocky crust. The upper solidifying layer was broken off on angular blocks with sharp ribs and stretched crosspieces between them. With the lapse of time, these crosspieces were broken off, creating an original completed blocky surface. In the quaternary lavas of the Armenian volcanoes, owing to weathering and frost action, the blocky lavas were subjected to disintegration, creating scatterings of blocks of the andesite-basalt, which has already lost the characteristic features of the real blocky lavas [3].

Many petrographs consider basalt magma to be the "parent" primary, from which all other eruptive rocks could occur by differentiation and also by contamination the more silicate-rich material of earth crust. Together with basalts, andesites, as is known, are the most widespread stone rocks. Basalts consist approximately equally of plagioclase and iron-magnesian minerals. Basalt structure is often zonal or sand-glass, medium and macro-crystalline and porphyritic. The microstructure of base mass is most often intersertal, microdoleritic is also quite common, ophitic is less common, and little-crystallized types with hyalopilitic and hyaloophytic structure are less extended.

Andesites are characterized by a macroscopically aphanitic base mass essentially consisting of lime-sodium plagioclase together with subordinated amount of pyroxene and some amount of glass. Such a base mass sometimes entirely builds up the whole rock, but is more often the base mass containing phenocrysts of lime-sodium plagioclase. More acidic plagioclases are characteristic for corniferous and mica andesites, more basic - for augitic. Phenocrysts, as a rule, are with the developed zonal structure and have common tablitic appearance. The zonal structure of plagioclase for andesites is characteristically more than for basalts [4].

Results

On the basis of microscopic study of rock sections, it is revealed that the rock consists basically of minerals opacitized hornblende and plagioclase (up to 30% of the rock). The hornblende pleochroes in red-brown tones, from ash-light-green to red-orange and yellow-red and is surrounded by an opacitic edge consisting of opaque small grains of magnetite. This mineral is represented by two generations of elongated narrow prismatic crystals: the first - with the sizes of 1.5... 4.5 mm, the second - less than 1.5 mm. Plagioclases are also represented by two generations, the first of which is porphyritic phenocrysts, in the form of short thick impregnations with the sizes 1.0... 2.0 mm, and the second generation - microlites with the sizes less than 1.0 mm.

The texture of the rock concerns type "massive". The rock structure is microporphyritic and porphyritic with the microlitic structure of the base mass. The relation of fine impregnations and fine-grained base mass is approximately the same and is 48% and 52%, respectively. Visually, the rock has no macrocracks, macro-crosses, and macrocracks are not found by microscopic studies on either opacitized prismatic phenocrysts hornblendec or on the surface of watery-transparent phenocrysts of plagioclase.

There are no secondary minerals in the rock, such as hydroxides of iron, chlorites, epidote, quartz, saricite, etc., xenoliths, xenocrysts and accessory minerals are also not found. There are no impurities of solid and loose minerals, there are no inclusions of quartz, silicon nodules, clay and other harmful rocks.

Table 1 shows the chemical composition of the stone, the content of which components is average value of the analysis of three samples of powder of ground rock.

Table 1. Results of the chemical analysis

The content of components, %							
SiO ₂	Al ₂ O ₃	TiO ₂	Fe ₂ O ₃	CaO	MgO	K ₂ O+Na ₂ O	SO ₃
60.18	17.49	0.61	5.78	5.63	2.55	6.29	0.29

Table 2 shows the results of the study of the main qualitative indicators of stone rock. Average values of density and strength were determined by testing 20 stone samples. Coefficients of water saturation, softening and frost resistance are average values of the corresponding indicators of three tests. In experiments on frost resistance, six control and nine basic cubes were used for each cycle of alternate freezing in the climate chamber and thawing in room conditions.

Table 2. Results of study of the main qualitative indicators of stone rock

Average density, kg/m ³	Average strength at compression, MPa	Coefficient of water saturation	Coefficient of softening, $K_{softening} = R'_{av.} / R_{av.}$	Coefficient of frost resistance at 100 cycles of tests
2192	76.4	0.46	0.869	0.96

Discussion

On the basis of petrographic researches, chemical and mineralogical compositions, structural and textural features of the material are revealed, analysis of which results has allowed to define that the studied stone rock is corniferous andesite.

Corniferous andesites, as is known, are characterised by a combination of the phenocrystals of plagioclase and hornblende, plagioclase with the impregnated biotite. In addition, pyroxene, mainly hypersthene, can be found, and to this sign andesites receive the name corniferous. The corniferous andesite, as a rule, is richer in silicate, that is visible on chemical composition of the material and has affected the microlite structure of the base mass. There are clearly expressed traces of opacitization of the hornblende, which explains the colour of the material. It is necessary to underline, that it is not connected with superficial low-temperature changes, with weathering. The phenomenon of hornblende opacitization can be explained as follows. At contact with air oxygen, the bivalent iron is oxidized to trivalent, the reaction causes the temperature of the andesite lava poured out on the surface to rise. At the same time around phenocrystals of hornblende there is formed opacitic edge, as a result of which green hornblende is painted in orange-red and brown colors.

The analysis of results of technological researches has shown that stone rock has density of 2.200 kg/m³ and strength of 76.4 MPa, which corresponds to the rocks of the andesite species. Coefficients of softening (0.869), water resistance (0.46) and frost resistance (0.96) testify to sufficiently high quality of stone rock, that allows to recommend the studied material for wide application in construction practice, including for external works.

Conclusion

The investigated natural stone material of the "Saralsk" deposit on its mineralogical and chemical composition is hornblende andesite. It consists of impregnated hornblende and plagioclase in the form of tabular porphyritic phenocrystals, smaller sheets and microlites. Rock-forming minerals of andesite are not subject to secondary changes, traces of weathering of the material are absent.

The hornblende andesite has a "massive" texture, the structure of the rock is microporphyritic and porphyritic with the microlite structure of the base mass. In rock are absent macro- and microcracks, are not found out impurities of secondary and harmful minerals.

The revealed basic technical characteristics of a stone testify to high quality of the material and sufficiently resistant to negative influences of environment.

The complex analysis of the results of petrographic and technological researches of stone rock of the "Saralsk" deposit has shown the suitability of hornblende andesite for practical application in construction, including for external works.

References

- [1]. Z.A. Atsagortsyan, Natural stone materials of Armenia. Stroyizdat, Moscow, 1967.
- [2]. L.V. Krasulina, Determination of the specific effective activity of natural radionuclides in building materials. BNTU, Minsk, 2014.
- [3]. V.A. Aghamalyan, O.A. Sargisyan, T.K. Lorsabyan, A.G. Israyelyan, Main tectonic units of Armenia, YSU scholarly notes. Geology Geography, 1, 2012, 3-12.
- [4]. A.N. Zavarickiy, Igneous rock. USSR Academy of Sciences, Moscow, 1960.

Avetik Artavazd Arzumanyan, doctor of philosophy (PhD) in engineering, associate professor (RA, Yerevan) - National University of Architecture and Construction of Armenia, lecturer at the Chair of Production of Construction Materials, Items and Structures, avetikarzumanyan@gmail.com

Vardan Grigor Tadevosyan (RA, Yerevan) - Horizon 95 Research Laboratory, senior specialist, vtadevosyan@gmx.de

Nelli Gagik Muradyan (RA, Yerevan) - National University of Architecture and Construction of Armenia, head of the Research Laboratory at the Chair of Production of Construction Materials, Items and Structures, nellimuradyan06@gmail.com

Navasardyan Hovhannes Vachagan (RA, Yerevan) - Horizon 95 Research Laboratory, engineer, navasardyan.hovo@mail.ru

Submitted: 01.02.2021

Revised: 15.03.2021

Accepted: 22.03.2021

UDC 691.31

DOI: 10.54338/27382656-2021.1-2

Maria Martin Badalyan^{1*}, Amalya Karapet Karapetyan¹,
Nelli Gagik Muradyan¹, Sona Sahak Ratevosyan²

¹ National University of Architecture and Construction of Armenia, Yerevan, RA

² HVAC-PD Engineers, Yerevan, RA

POSSIBILITY OF TUFF WASTE APPLICATION IN THE PRODUCTION OF THERMAL INSULATION MATERIALS

Possible methods of dust, sand and gravel waste involvement during tuff mining for production of modern thermal-insulating construction materials using energy-efficient technologies are presented. The possibility of using the valuable properties of these wastes for the production of modern competitive materials and products, particularly clinkerless binders, artificial porous fillers, foam concrete, etc is described. The volcanic rocks, which have a glass-like structure, i.e. easily modified, give the system sufficient energy potential, which is accumulated in the rock, allowing work to be performed through chemical reaction. The possibility of increasing rock reactivity both by mechanical (crushing, grinding) and chemical methods (creation of basic, sulfate environments) is presented.

It has been theoretically substantiated and practically confirmed that by using the waste materials it is possible to obtain artificial construction conglomerates of various structures using resource-saving technologies and the activities of rocks endowed with nature. The composition of concrete with a cellular structure has been developed and its physical and mechanical characteristics have been brought forth.

Keywords: tuff waste, energy-efficiency, rock activity, inner energy, specific surface, lime-sand binder, environmental issues, low-basic hydrosilicates and hydroaluminates, heat resistance.

Introduction

Armenia has large resources of different types of mountain rocks, which, however, are limited; it is necessary to look for ways to use them rationally and effectively. Mining and processing of mountain rocks generate large amounts of waste, which creates serious environmental problems that are constantly intensifying. In particular, the mining and processing of tuff rock generate a large amount of waste, the disposal of which is of great economic and environmental importance [1].

About 60-80% of the mined tuff mass turns into waste, which is due to the cracks of natural tuffs. As a result, a large amount of waste, such as dust, sand and gravel accumulates around the mine, which pollutes the environment and causes serious environmental problems. These wastes are subjected to alkalinization under the influence of atmospheric factors and become a constant pollution source for air, underground water and surface water. Irrigation of land by these waters leads to salinization of land, the regeneration of which requires considerable costs. These wastes are very cheap, but valuable raw materials for the production of modern competitive materials and products, especially clinkerless binders, foam concrete of solid and cellular structure, artificial porous fillers, etc. [2-4].

Main Part

The complex use of mineral raw materials, particularly tuffs, has been and remains a very relevant problem, which is connected with the large amounts of waste generated.

Our republic has a rich raw material base for the production of effective thermal insulation materials, but up to this day such materials are imported from abroad, resulting in a significant increase in their cost. Moreover, the properties of thermal insulation materials and products deteriorate during transportation due to their low strength or fragile structure, and the load-carrying capacity of the vehicle is not fully utilized, as these

materials have low average density. Therefore, it is necessary to find ways to organize the production using material and energy-efficient technologies involving various types of industrial waste, which are available in the country in millions of cubic meters and are dangerous in their nature. By involving this waste as the main raw material for the production of thermal-insulating materials and products, it will be possible to reduce the mining of precious mountain rocks, by making the use of natural resources more rational. Thermal-insulating materials are used not only in construction, but also in various areas - for insulation of pipelines, chemical machinery, thermal units, which increases their productivity.

It should be noted that special attention should be paid to the thermal insulation of refrigerators, since the cost of a refrigeration unit is approximately 20 times more expensive than the cost of the corresponding thermal unit [5,6].

Thus, the one effective way of scientific and technological progress is to involve wastes into circulation, which are one of the sources of environmental pollution.

The use of industrial wastes and secondary materials as the main raw material in the production of various construction materials and products contributes to the creation of low-waste or waste-free technologies and at the same time solves social problems, particularly of environmental protection.

On the basis of the above mentioned, the task was set to study the possibility of obtaining effective competitive thermal-insulating materials and products from tuff waste by energy-efficient technological schemes.

The tuff rocks have a glass-like structure, that is, there are crystalline enclosures in the amorphous body, and when these enclosures leave the center, the regular structure is gradually disrupted, giving the rock sufficient energy potential. Thus, rocks with volcanic glass structures are mutable (amorphous), i.e. they can be easily changed, which gives the system sufficient energy potential to work through chemical reactions. Mechanical methods (crushing, grinding) and chemical methods (creating basic sulfate environments) can be used to increase the reactivity of the rocks.

Mountain rock crushing severely disrupts the surface of the particles, resulting in a large number of unsaturated surface bonds. These surface disruptions significantly increase the activity of the materials compared to the original. As the specific surface of the material increases, surface energy also increases, but over time the surface charges neutralize, which leads to a decrease in surface energy and an increase in the inertia of the rock.

Although, according to the Gibbs-Curie principle, an increase in the degree of the material grinding leads to an increase of its solubility and chemical activity [1, 2, 7], the energy potentials increase so much from a certain index of grinding fineness, that a spontaneous aggregation of particles takes place, which leads to a reduction in the specific surface area of the original material. Similar phenomena have been observed in the study of disperse systems based on volcanic rocks [1, 2, 8], and those phenomena have been explained by the fact that with a high degree of grinding fineness, the regulation degree of the volcanic glass structure increases: the mutable state shifts to a metastable (changing-stable) and to a more stable crystalline form (Table 1). Limitations must therefore be imposed on rock grinding and to determine the fineness of grinding each type of volcanic rock experimentally. The optimum grinding rate depends on the chemical activity of the rock: the higher the activity index, the lower the rate of optimum grinding degree of the powder-like material, that is, in the case of a smaller specific surface area of a material, the aggregation of its particles begins.

Under certain conditions, rock energy can be used to synthesize waterproof conglomerates at relatively low temperatures. The criterion of reaction heat is enthalpy, and in case of exothermic reaction the reduction the enthalpy of the system, i.e. free energy is the driving force of the chemical reactions, and entropy increases, i.e., the disorder in the system decreases, which requires additional energy consumption. During the reactions in volcanic aluminosilicate rocks such disorders occur to some extent, which contribute to the production of silicate construction materials by energy-efficient technology.

The specific surface of the original materials together with the hydrothermal treatment regime can have a decisive impact on the phase composition of the new formations, which are crystallizing at the first phase of the synthesis. In the case of small dispersions of original material, low basic hydrosilicate of C-S-H (I) type is formed in two stages. In the first stage, bibasic calcium hydrosilicates are crystallized, which synthesize until all lime is bound, followed by the second stage, during which bibasic calcium hydrosilicates are dissolved and stable low-basic calcium hydrosilicate crystals are formed. At high dispersion rates of the silica-soil component, due to the high activity of its surface, high-basic hydrosilicate is not synthesized even at the stage of temperature increase.

Table 1. Evaluation of tuff rock activity by the amount of absorbed lime (mg/g)

Types of tuffs	Specific surface, m ² /kg		
	200	400	700
Ani	74.6	140.4	57.3
Artik	54.5	73.8	56.1
Aghavnatun	78.1	155.4	56.5
Kosh	79.4	146.4	55.7
Jrvezh	80.2	153.3	55.2
Armavir	70.8	136.6	52.5

The kinetics of silicate formation and the phase composition of new formations are strongly influenced by various additives, for example, mixtures containing aluminium. In this case, there is an increase in strength, which is explained by an increase in the density of the monolith and in the number of new formations. If there is clay soil in the system, the mechanism of silica formation changes. In this case, first hydroaluminates are synthesized, then calcium hydrosilicates [2, 8].

The synthesis of calcium hydrosilicates by the CaO-SiO₂-H₂O system is well covered in the reference. Scientific works by Yu.M. Butt, A.N. Rashkovich, Yu.P. Gorlov and Armenian scientists M.H. Badalyan, L.G. Kalashyan and others are dedicated to it. Similar systems are R₂O-SiO₂-H₂O slug-alkaline systems, which were developed in Ukraine by Glukhovsky V.D. [5, 6, 9, 10].

On the basis of all the developed scientific concepts it has been established that synthetic processes in the earth's crust are similar to processes in industrial conditions, but differ in activation of output components, which, without changing the essence of mineral formation, affects only the duration.

During structural operation, energy efficiency should be taken into account as well. One of the biggest consumers of fuel and energy resources is the utility-household sector. In Armenia, from 2 to 3 times [2] more conventional fuel is spent on heating buildings than for the same purposes in developed countries, and the reason is the non-strict thermal physical requirements for wall materials. Even in new buildings wall materials do not meet strict requirements for thermal resistance.

The traditional wall materials used in Armenia were blocks of mountain tuff rocks for decades, which are not expedient for use as wall material today, as the requirements for thermal resistance have become stricter in modern building standards - HShN II-7.02-95 [11]. The normative indicators of thermal resistance can be provided only in case of 0.9... 1.2 m thick tuff wall. The triple increase in the wall mass, together with the drastic increase in the construction cost, will lead to a significant deterioration of the seismic resistance of the objects under construction.

Products and structures made of autoclaved aerated concrete meet these requirements most. Thanks to the long-term hard work of the Armenian scientists, the technologies for obtaining autoclaved aerated concrete from local raw materials have been developed [12]. Since Armenia is located in a seismically active zone, products made of light autoclaved aerated concrete will increase the seismic resistance of structures by reducing the weight of buildings and structures.

In addition to the technical and economic indicators, wall materials are also evaluated on other indicators, for example, comfort. According to the classification of wall materials in terms of comfort, wooden walls are in the first place, houses with autoclaved aerated concrete walls are in third place, walls of silicate and ceramic brick are in 6-9 places, and reinforced concrete is in last place [4]. Autoclaved aerated concrete house is very close to a wooden house in its operation, but does not burn. It is a material with a great perspective, as it has sufficient strength (5MPa), is easily processed and it is possible to get products of any geometric shape and size [13].

The cellular structure improves the sound insulation properties, which is very important for residential building construction. Besides these important parameters, autoclaved aerated concrete “breathes”, it can be sawn, it is able to regulate humidity in the apartment, eliminates the possibility of fungus growth, does not rot, because it is produced from mineral raw material, is environmentally friendly and does not contain dangerous chemical compounds. All these characteristics give reason to consider aerated concrete as one of the best building materials of the 21st century [13]. Aerated concrete is widely used in the West and CIS, where most of them are produced with German equipment [4, 5].

Raw material for the production of building materials should be widespread and environmentally friendly. In nature it is water, carbonate rocks (limestone, chalk, marl) and products of their processing - lime concrete, etc. Comprehensive analysis of radiation safety of raw materials and construction products showed the advantages of using silicate products in residential construction.

Aerated concrete blocks are often produced of lime-sand binder (such as quartz sand) and are reinforced in autoclaves. If the aluminosilicate component is active, the reinforcement process can be performed using energy efficient technology in a heat-moisture processing chamber [2, 8]. Taking into account the requirements for the strength of the blocks and the fact that the Portland cement blocks still have higher strength, during the study it was envisaged to use a mixed lime-cement binder, i.e., partially replace the expensive Portland cement with less energy-consuming lime-sand binding (240 kg of conventional fuel is used to obtain 1 ton of Portland cement, and 160 kg of conventional fuel for 1 ton of lime) [2, 14].

The binding powder obtained as a result of joint grinding of crystalline silicate component and lime, with a certain ratio is considered clinkerless, because without an aluminosilicate component, lime is an air-binder. Kosh mine tuff wastes have been used for studies, as this type of tuff is highly active (Table 1). Mixed binder compositions have been developed, where the ratio of binder-aluminosilicate component is 1:3, not taking into account that the fraction of sand dust is in the composition of the lime-sand binder. The obtained results are presented in Table 2.

The heat-moisture treatment was carried out with steam heating up to 95 °C in the following mode: 3 hours of temperature increase, 8 hours of isothermal treatment and 3 hours of temperature decrease. After heat-moisture treatment, the samples were dried in laboratory conditions and tested.

Table 2. Physical and mechanical parameters of autoclaved aerated concrete based on quicklime and Kosh mine tuff

Quicklime, %	Cement, %	Gypsum, %	Aluminium powder, %	Physical and mechanical properties	
				density, kg/m ³	Compressive strength limit, MPa (class)
10	10	-	0.02	916	2.2 (B1.5)
10		2.5		940	7.2 (B 5)
15		2.5		938	7.8 (B 5)
15		5.0		944	8.4 (B 5)
10		-	0.03	876	1.9 (B1.5)
10		2.5		890	6.2 (B 5)
15		2.5		894	6.5 (B 5)
15		5.0		895	7.1 (B 5)

Gypsum in the system is an additive or sulphate activator, the presence of which sharply increases the process of hydrolysis of volcanic rock, alkaline extraction of the soluble alkali component, which leads to a drastic increase in condensation of the system.

The alkali, being electrolytes, increase the ionic potential of the solution, enriching it with OH⁻ ions, thereby increasing the solubility of the system's original materials, contributing to the formation of silica gel.

Conclusion

The high strength of lime-aluminosilicate binding material is conditioned by physical and chemical processes that occur in the system and lead to the formation of cement stone. The composition of these new formations depends on the CaO and SiO₂ ratio, the fineness of the grinding, the structure of the aluminosilicate component and the temperature of reinforcing.

Low basic calcium hydrosilicates and hydroaluminates are mainly formed by heat-moisture treatment. Calcium hydrosilicate from hydrolysis of cement alite mineral - Ca(OH)₂, can also be involved in the formation process of structure-forming by chemically binding to the active silica soil and alumina soil in the system, bringing forth new formations of tobermorite and hydrogranate type. The structure of the aluminosilicate component is very important, because the temperature of the chemical binding capacity of lime depends on the structure.

Autoclaved aerated concrete is one of the wall materials with the best properties of the 21st century, which can meet the requirements of thermal resistance, reducing the mass of the structure. It can be produced with various binders, including clinkerless, mixed, cement, which can be produced with the involvement of tuff waste as the main component, present in large quantities in our country. In addition, the cellular structure contributes to the improvement of sound insulation properties, which is very important for residential construction.

References

- [1]. V.I. Barkhatov, I.P. Dobrovol'skiy, Yu.Sh. Kapkaev, Otkhody proizvodstv i potrebleniya – rezerv stroitel'nykh materialov. Chelyabinskiy gosudarstvennyy universitet, Chelyabinsk, 2017.
- [2]. M.M. Badalyan, A.K. Karapetyan, L.M. Ter-Oganesyan, Vovlechenie otkhodov nerudnoy promyshlennosti v proizvodstvo stroitel'nykh materialov i izdeliy. Krizisnoe upravlenie i tekhnologii. Mezhdunarodnaya konferentsiya, Nov. 12-13, 2 (15), 2019, 179-185.
- [3]. P.A. Ter-Petrosyan, M.M. Badalyan, Badalyan M.G., Israelyan V.R., Cementless concrete is a perspective material for construction seismic resistance. Bulletin of Builders of Armenia (special issue), 6, 1997, 17-18.
- [4]. N.P. Sazhnev, Sazhnev, N.N., Galkin S.L., Experience in the production and use of aerated concrete products of autoclave hardening in the Republic of Belarus. Building materials, 1, 2008, 6-10.
- [5]. V.D. Glukhovskiy, Runova R.F., Sheinich L.A., Gelevera A.G., Fundamentals of the technology of finishing, heat- and waterproofing materials. Higher school, Kiev, 1986.
- [6]. Yu.P. Gorlov, Technology of heat-insulating and acoustic materials and products. Higher school, Moscow, 1989.
- [7]. R.G. Dolotova, V.N. Smirenskaya, V.I. Vereshchagin, Evaluation of the activity of low-silica raw materials and their suitability as aggregate for concrete. Building materials, 1, 2008, 40-42.
- [8]. M.M. Badalyan, Cementless concretes based on raw materials from Buryatia. Bulletin of Builders of Armenia (special issue), 8, 1999, 8-9.
- [9]. V.D. Glukhovskiy (Ed-in-chief), Use of industrial waste and a comprehensive solution to the problem of building materials, Materials of the 3rd scientific conference on problems of increasing production efficiency and development of productive forces of the Komi Republic, Syktyvkar, 1973.
- [10]. V.D. Glukhovskiy, P.V. Krivenko, V.N. Starchuk, I.A. Pashkov, V.V. Chirkova, Slag-alkali concretes on fine-grained aggregates. Higher school, Kiev, 1986.

- [11]. M.M. Badalyan, Expediency of the use of aerated concrete in the conditions of the Republic of Armenia. Union of Builders of Armenia, Bulletin Collection of Scientific Works, 1, 2015, 50-54.
- [12]. V.N. Myasnikov, Aerated concrete - material of the XXI century. Industrial and civil construction, 7, 2001, 34.
- [13]. V.A. Pinsker, V.P. Vylegzhanin, Ways of saving cement in the production of aerated concrete. Building materials, 1, 2008, 43.

Maria Martin Badalyan, doctor of sciences (engineering), associate professor (RA, Yerevan) - National University of Architecture and Construction of Armenia, acting head of the Chair of Production of Construction Materials, Items and Structures, marya.badalyan@mail.ru

Amalya Karapet Karapetyan, doctor of philosophy (PhD) in engineering, associate professor (RA, Yerevan) - National University of Architecture and Construction of Armenia, lecturer at the Chair of Production of Construction Materials, Items and Structures, shinnyuter@gmail.com

Nelli Gagik Muradyan (RA, Yerevan) - National University of Architecture and Construction of Armenia, head of the Research Laboratory of the Chair of Production of Construction Materials, Items and Structures, nellimuradyan06@gmail.com

Sona Sahak Ratevosyan (RA, Yerevan) - HVAC-PD Engineers, design engineer, sona.ratevosyan@mail.ru

Submitted: 04.02.2021

Revised: 17.05.2021

Accepted: 24.05.2021

UDC 624.04.531.3

DOI: 10.54338/27382656-2021.1-3

Valeriy Peter Bondarenko

Don State Technical University (DSTU), Rostov-on-Don, RF

FORMATION OF STIFFNESS MATRICES OF PLANE ELEMENTS BASED ON HIGH-ORDER DEGREE POLYNOMIALS

In this paper, the method for forming the stiffness matrix of a plane element in a plane stress-strain state using functions approximating the displacements of the points of the element in the form of high-order degree polynomials is considered.

Keywords: *stiffness matrix, Ritz method, stress-strain state, potential strain energy.*

Introduction

When calculating structures using the finite element method, a solid area is represented as an area consisting of a number of smaller areas, called finite elements. To approximate the point displacements of the finite rectangular or triangular element, linear functions are usually used to ensure the continuity of deformations in the nodes and along the edges of the junction of finite elements. In order to increase the accuracy of the solution, the number of finite elements into which a solid area is divided increases, resulting in a significant increase in the order of the system of solving equations.

When calculating a lamellar structure, for example a large-panel building, the main structural elements of which are plane rectangular elements (wall panels, partition panels, floor and roof slabs), a typical structural element of a large-panel building can be taken as a finite element.

Since during the assembly of a large-panel building the main docking of its elements is carried out at nodal points, when selecting functions approximating the displacement of points of the element, it is not necessary to ensure conditions of continuity of deformations along the edges of structure element dockings. This allows using nonlinear functions as approximating functions, for example, high-order degree polynomials. The basic provisions of this methodology are described in [1-3].

Stiffness Matrix of a Plane Element Based on High-Order Polynomials

In the work [4], the stiffness matrix of a plane rectangular plate was obtained, operating according to the beam-wall scheme, loaded with concentrated forces applied at the nodal points of the plate free from bonds. The problem was solved by the Ritz variation-energy method. To approximate the displacement functions of an arbitrary point, degree polynomials of the following type were taken:

$$\begin{aligned} u_1 &= f_1(x, y) \sum_{m=0}^K \sum_{n=0}^K \alpha_{mn}^I x^m y^n; \\ u_2 &= f_2(x, y) \sum_{m=0}^K \sum_{n=0}^K \alpha_{mn}^{II} x^m y^n, \end{aligned} \quad (1)$$

where

$K = (m+1) \cdot (n+1)$ – number of members of the series to be retained;

$f_1(x, y)$ and $f_2(x, y)$ – functions that meet kinematical boundary conditions (conditions for fixing the plate as a completely solid body).

The accuracy of the solution was achieved by increasing the number of retained members of series. In this case, the dimension of the obtained stiffness matrix remained constant.

In the finite element method, the elements into which the structure is divided are outwardly kinematically free. In order to use the considered plate as a finite element of the system, we will free it from bonds and allow it to move in its plane, as an absolutely stiff body (Fig. 1).

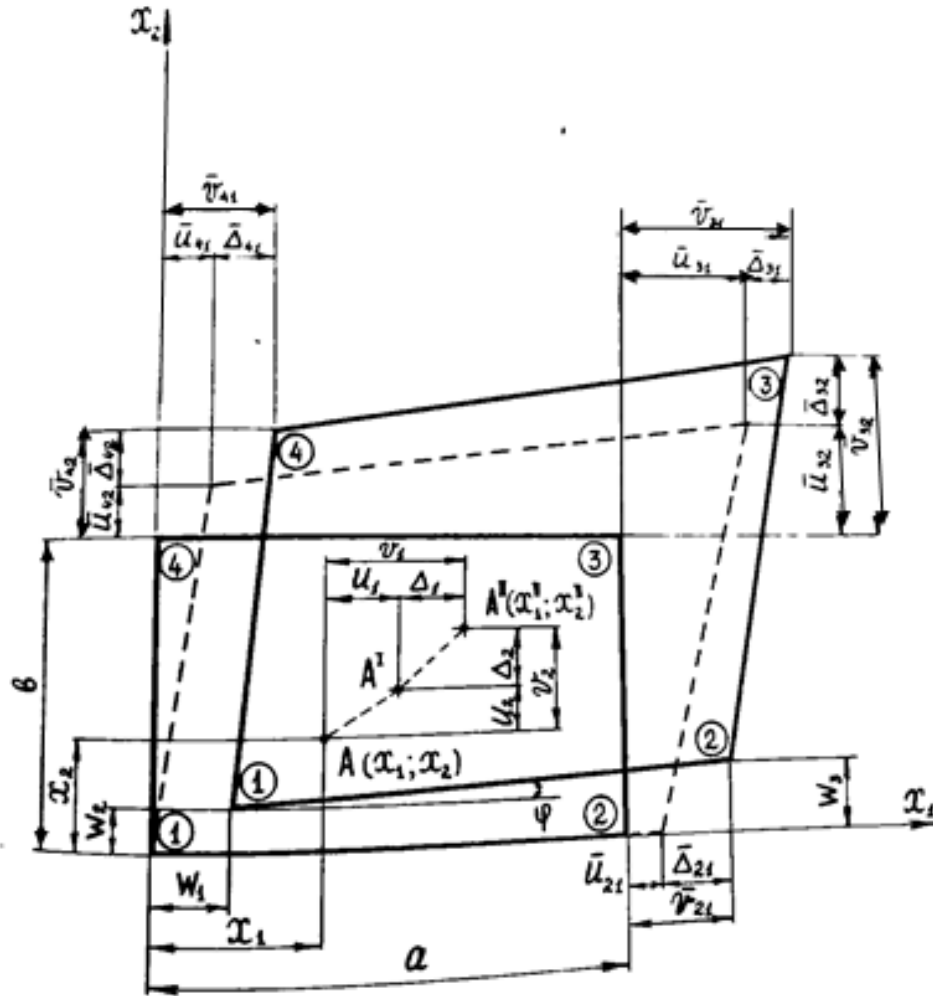


Fig 1.

Here

u - displacements of the arbitrary point caused by elastic deformations;

Δ - additional displacements of the arbitrary point caused by the displacement of an element as an absolutely solid body;

v - full displacements of the arbitrary point;

w_1, w_2, w_3 - components of the "rigid" displacement of the plate.

During small displacements

$$\operatorname{tg} \varphi = \varphi = (w_3 - w_2) / a.$$

The total displacements of the arbitrary point $A(x_1, x_2)$ inside the plate will consist of displacements caused by elastic deformation and additional displacements caused by the displacement of the plate as an absolutely solid body:

$$\{v\} = \{u\} + \{\Delta\}. \quad (2)$$

$$(2 \times 1) \quad (2 \times 1) \quad (2 \times 1)$$

The vector of elastic displacements $\{u\}$ was obtained in [4].

Additional displacements Δ are expressed through w displacements according to the known ratios of analytical geometry (Fig. 2).

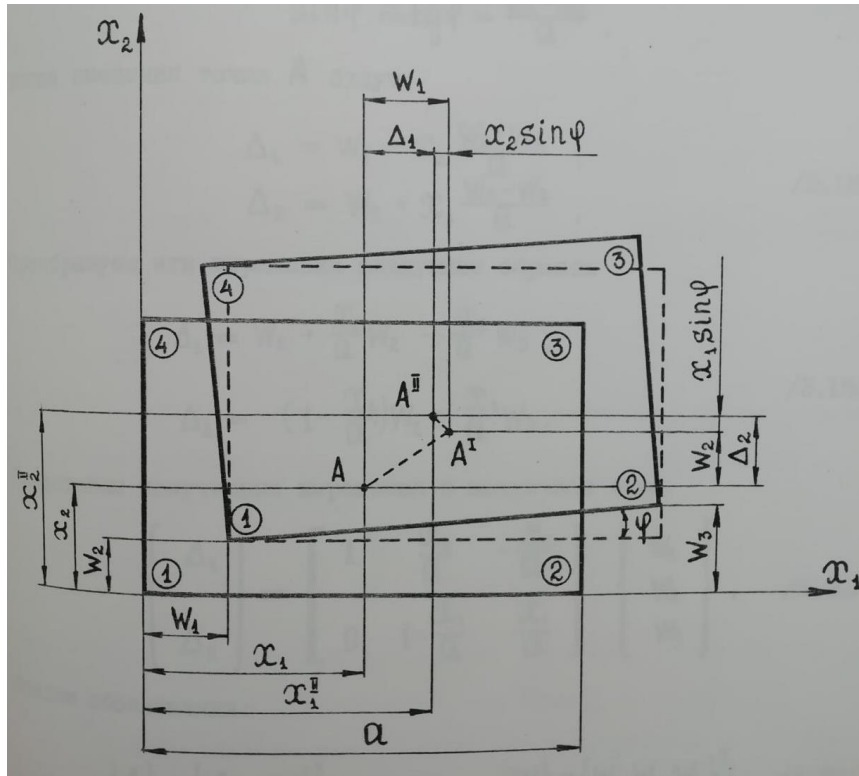


Fig. 2.

The displacement of the considered point A after displacement of the plate as an absolutely solid body will be equal to:

$$\begin{aligned}\Delta_1 &= x_1^H - x_1 = w_1 + x_1 \cos \varphi - x_2 \sin \varphi - x_1 = w_1 - x_2 \sin \varphi - x_1 2 \sin^2 \varphi / 2; \\ \Delta_2 &= x_2^H - x_2 = w_2 + x_1 \sin \varphi + x_2 \cos \varphi - x_2 = w_2 - x_1 \sin \varphi - x_2 2 \sin^2 \varphi / 2.\end{aligned}\quad (3)$$

Taking into account the smallness of the angle φ , it is possible to neglect the sizes of the second order of smallness in expression (2) and, besides, to accept

$$\sin \varphi \approx \operatorname{tg} \varphi = (w_3 - w_2) / 2.$$

Then the expressions for the displacement of point A can be recorded as follows:

$$\begin{aligned}\Delta_1 &= w_1 + x_2 w_2 / a - x_2 w_3 / a; \\ \Delta_2 &= (1 - x_1 / a) w_2 + x_1 w_3 / a.\end{aligned}\quad (4)$$

Let us represent the resulting equations in matrix form:

$$\{\Delta\} = [Z_D] \cdot \{w\}.\quad (5)$$

Here the matrix $[Z_D]$ of dimension (2×3) has the following form:

$$[Z_D] = \begin{bmatrix} 1 & x_2 / a & -x_2 / a \\ 0 & 1 - x_1 / a & x_1 / a \end{bmatrix}$$

Put the obtained expressions for $\{u\}$ and $\{\Delta\}$ in formula (1):

$$v = [Z] \cdot \{U\} + [Z_v] \cdot \{w\}.\quad (6)$$

$$(2 \times 1) \quad (2 \times 3) \quad (5 \times 1) \quad (2 \times 3) \quad (3 \times 1)$$

After a simple transformation, expression (5) is represented as:

$$\{v\} = [Z_d] \cdot \{p\}, \quad (7)$$

$$(2 \times 1) \quad (2 \times 8) \quad (8 \times 1)$$

where $\{p\}$ - a vector, the elements of which are "elastic" displacements of unfixed nodes of the plate and three independent displacements of this plate as an absolutely solid body.

$$\{p\} = \{u_{21} \ u_{31} \ u_{32} \ u_{41} \ u_{42} \ w_1 \ w_2 \ w_3\}^T. \quad (8)$$

By setting the coordinates of the nodal points in formula (4), the total nodal displacements are expressed through the vector $\{p\}$:

$$\{V_0\} = [M] \cdot \{p\}. \quad (9)$$

$$(8 \times 1) \quad (8 \times 8) \quad (8 \times 1)$$

Matrix $[M]$ is obtained from consideration of the geometric scheme of displacements. The vector $\{p\}$ is determined from expression (8):

$$\{p\} = [M]^{-1} \{V_0\}. \quad (10)$$

By putting the expression (9) into formula (6), we will obtain the value of the displacements of the arbitrary point of the plate through the displacements of its nodes:

$$\{v\} = [Z_n] [M]^{-1} \{V_0\} \quad \text{or} \quad \{v\} = [Z_0] \{V_0\}, \quad (11)$$

$$(8 \times 1) \quad (8 \times 8) \quad (8 \times 1)$$

where $[Z_0] = [Z_n] [M]^{-1}$ is the so-called coordinate matrix.

Expressing all the components of the stress-strain state of the arbitrary point of the plate through the displacements of its nodes, we make up the functional of the total potential energy of the deformation of a rectangular flat plate having 8 degrees of freedom and loaded with a system of nodal concentrated forces.

Minimizing the functional of the potential deformation energy through nodal displacements, we come to a system of algebraic equilibrium equations:

$$\frac{Eh}{1-\nu^2} [T] \cdot \{U\} = \{F\}. \quad (12)$$

$$(8 \times 8) \quad (8 \times 1) \quad (8 \times 1)$$

Here

E and ν – elastic constants of the material;

h – plate thickness;

$\{F\}$ – vector of nodal concentrated forces.

Rectangular symmetric matrix $[T]$ is the stiffness matrix of the standard element:

$$[T] = \iint [S]^T [\mu] [S] dx_1 dx_2. \quad (13)$$

Here $[S]$ and $[\mu]$ - matrices obtained by forming an expression for the potential energy of deformations in matrix form.

The general algorithm for calculating the elements of the stiffness matrix is represented by the formula:

$$t_{ij} = \iint [(s_{11} + \mu s_{22}) s_{1j} + (\mu s_{11} + s_{22}) s_{2j} + \frac{1-\mu}{2} s_{3i} s_{3j}] dx_1 dx_2. \quad (14)$$

Conclusion

The stiffness matrix of the element obtained by the given algorithm depends on the degree of approximation of the displacement functions. The desire to obtain a more accurate solution will require the preservation of a larger number of members of the series (1).

In traditional FEM, the refinement of the solution is achieved by dividing the solid area into smaller parts or by assigning a greater number of node points to the finite element. But if in the FEM this leads to an increase in the size of the stiffness matrices, then they have a constant dimension regardless of the number of retained members of the series in the displacement functions.

This allows taking relatively large structural elements of large-panel buildings and other prefabricated structures as basic finite elements, which makes it possible to significantly reduce the order of the resolving system of equations formulated for the entire structure.

References

- [1]. R. Gallager, Metod konechnykh elementov. Osnovy. Mir, Moscow, 1984 (in Russian).
- [2]. B.A. Postnov, S.A. Dmitriev, B.K. Eltishev, A.A. Podionova, Metod syperelementov v raschetah inzhenernykh sooruzheniy (ed. V.A. Postnova). Sudostroenie, Leningrad, 1979 (in Russian).
- [3]. A.M. Sapozhnikov, Metodi syperelementov v statike i dinamike panelnykh sdaniy. Stroitelstvo i arhitektura. Izv. VUZov, 9, 1980 (in Russian).
- [4]. V.P. Bondarenko, Raschet konstruktivnykh elementov krupnopanelnykh zdaniy variatsionnym metodom Ritca. Nauchnoe obozrenie: Izdatelskiy dom "Nauka obrazovaniya". 11 (2), 2014, 450-452 (in Russian).
- [5]. V.P. Bondarenko, Raschet prymougolnoy plastinki metodom Ritca, Issledovaniya po raschetu plastin i obolochek. Rost. inj. - stroit. in-t, Rostov n/D, 1982, 101-108 (in Russian).
- [6]. B.A. Kositsyn, Sticheskiy raschet krupnopanelnykh i karkasnykh sdaniy. Isdatelstvo literatury po stroitelstvu, Moscow, 1971 (in Russian).
- [7]. G. Korn, T.Korn, Spravochnik po matematike. Dlya nauchnykh rabotnikov i inzhenerov. Nauka, Moscow, 1974 (in Russian).
- [8]. O.C. Zienkiewicz, The finite element method. Mc. Graw - Hill, London, 1967.

Valeriy Peter Bondarenko, doctor of philosophy (PhD) in engineering, associate professor (RF, Rostov-on-Don) - Don state technical University (DSTU), associate professor at the Chair of Strength of Materials, vb06402@gmail.com

Submitted: 11.01.2021

Revised: 10.02.2021

Accepted: 17.02.2021

Victor Dmitriy Eryomin

*Don State Technical University (DSTU), Rostov-on-Don, RF***ON NATURAL OSCILLATIONS OF A THIN ELASTIC WAVY SHELL OF AN OPEN PROFILE**

The article touches upon the problem of natural oscillations of a thin elastic wavy shell of an open profile. The proposed method for determining the numerical values of the lowest frequencies and the corresponding forms of natural oscillations of shells of a complicated shape is based on the Rayleigh-Ritz energy method.

The results of numerical calculation of this thin wavy shell with a hinge-fixed attachment along the lower contour along the generatrix are presented.

Keywords: wavy thin elastic shell, the frequency and form of natural oscillations, the energy method.

Introduction

The experience of construction in our country and abroad increasingly points to prospects of using shells with a complicated form, including wavy shells, as coatings of public, industrial, warehouse and agricultural buildings and structures.

The creation of new, more advanced engineering structures led to the necessity to develop the theory of calculation of shells with a complex shape: layered and corrugated, wavy and supported by a rod set.

The theory of thin shell calculation is well developed, so it is possible to calculate and then design the installations and structures in the form of shells of rather complex outlines.

However, in many cases they are exposed to periodic and impulsive loads, especially in seismic areas, so it is practically very important to have a simple mathematical apparatus to determine own frequencies of shells with complex geometry and natural oscillation forms corresponding to them.

By analyzing scientific works on the dynamics of shells, it is easy to notice the presence of a relatively small number of studies on calculation of natural oscillations of shells of nonclassic form.

The method of determination of numerical values of the lowest frequencies and natural oscillations of thin shells of complex shape corresponding to them by the energy method is proposed, which is acceptable for use in design practice.

This method allows replacing the differential equations with a uniform system of linear algebraic equations, which greatly simplifies the dynamic calculation of a shell of complex structure. As a particular case, this technique is applied for calculating smooth shells with any boundary conditions.

Task Setting

The problem of determination of numerical values of the lowest frequencies and natural oscillations of thin elastic wavy shell rectangular in plan with hinge-fixed attachment along the lower contour along the generatrix is considered (Fig.1).

Cross - section of the medial surface of the shell (by crest) is outlined by a curve, the equation of which is:

$$\frac{x^2}{a^2} + \frac{y^3}{b^3} = 1 \quad (1)$$

Medial surface of the shell is formed by curve movement

$$\alpha = -\Delta \left(1 - \cos \pi \frac{z}{\ell}\right) \quad (2)$$

along two adjacent crests of the shell and located in the normal flatness towards them. Here Δ is the cosine wave amplitude.

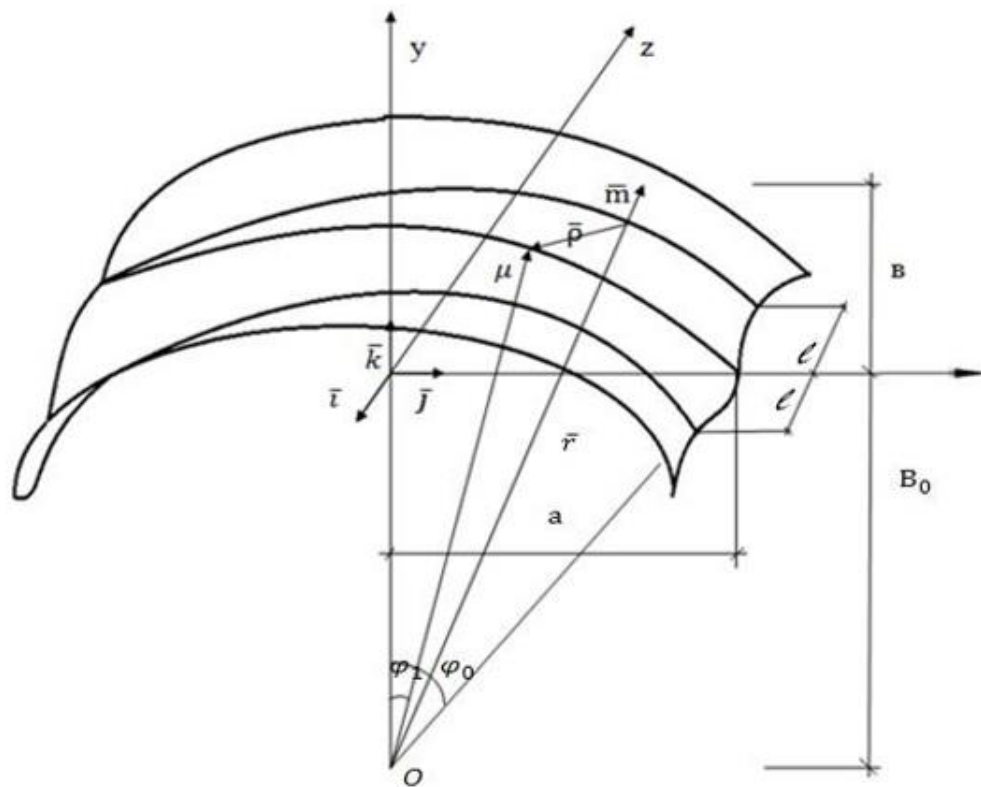


Fig. 1.

Geometric Characteristics (shell sizes)

Span - $2a = 18$

Height in cross-section passing through the crest of the shell - $h = 5m$.

Wavelength - $2\ell = 3m$.

Wave amplitude - $\Delta = 0.225m$.

Pole distance - $B_0 = 9m$.

Shell thickness - $2h = 0.05m$.

Physical Characteristics:

Shell material elasticity module - $E = 28HPa$

Poisson's ratio - $\mu = \frac{1}{6}$.

Shell material density - $\rho = 2500kg/m^3$.

Goal of the Paper

Obtaining numerical values of the lowest frequencies and natural oscillations of thin elastic wavy shell rectangular in plan corresponding to them (Fig. 1), with hinge-fixed attachment along the lower contour along the generatrix with coordinate $\alpha_2 = \pm 1$ (Fig.2).

The energy method of Ritz-Relay is the basis of the proposed methodology for determining the lowest frequencies and natural oscillation forms of complex shells corresponding to them. This method allows to obtain sufficiently precise values of the lowest frequencies and natural oscillations of complex shells corresponding to them under arbitrary conditions of fixation and under any law of changes in its geometric and physical characteristics. The main provisions of this methodology are outlined in [1-12].

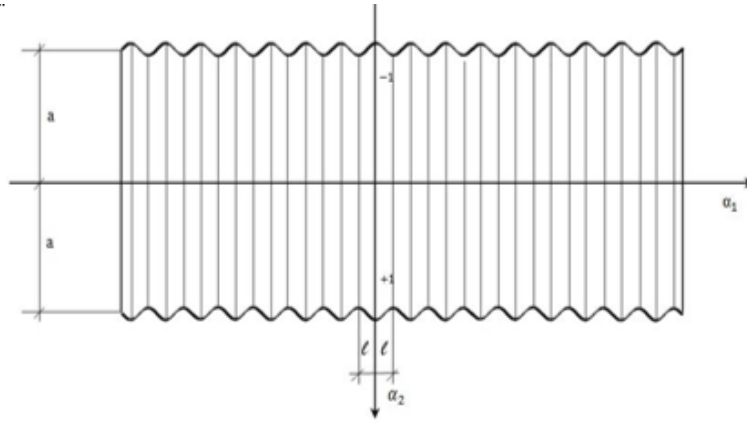


Fig. 2.

Calculation is based on geometric and physical linearity using Kirchhoff-Love hypothesis. It is assumed that the length of the shell along the Z axis (Fig.1) is rather large, so it is possible to limit the examination to the middle parts of it, without taking into account the influence of the shell parts adjacent to its ends.

Vector equation of the median surface of this wavy shell is obtained. Formulas for calculating parameters of Lamé and Christoffel symbols of this shell are displayed [6].

Functions approximating amplitudes of movement of points of the median surface of the shell along curvilinear axes of coordinates, in the form of double trigonometric rows, satisfying the conditions of hinge-fixed attachment of the shell along the lower contour along the generatrix are selected, as $\alpha_2 = \pm 1$: $u_1^0 = u_2^0 = u_3^0 = 0$ (Fig.2).

According to the formulas given in [7], matrices necessary for determination of numerical values of lower frequencies and natural oscillations of the given wavy shell are obtained.

Numeric Example Solution

The control of numerical convergence of the proposed algorithm calculation of the wavy shell is shown in Fig. 1, was carried out by the method of successive approximations, by stepwise increasing the number of members of the row approximating the solution.

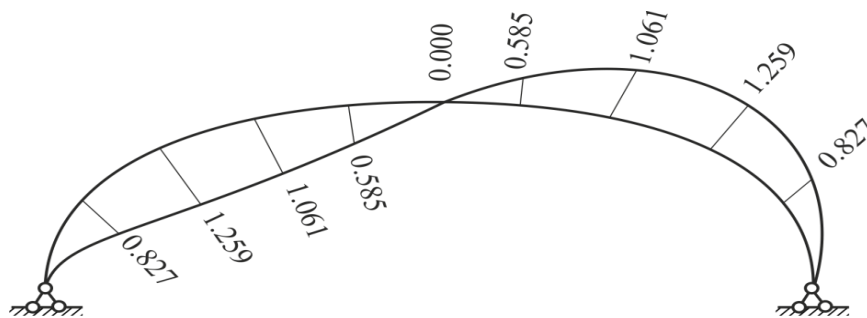
In the first approximation in double trigonometric rows approximating the movement, four members have been left ($m=n=2$), in the second approximation – nine ($m=n=3$), then sixteen ($m=n=4$), twenty five ($m=n=5$) and finally thirty six members in the row ($m=n=6$). Comparing the last three approximations in $m=n=4;5;6$, we will get convergence of results sufficient for engineering calculations.

The results of calculating the first two frequencies and forms of natural oscillations of the wavy shell with hinge-fixed attachment along the lower contour corresponding to them are shown in graphs 1-14.

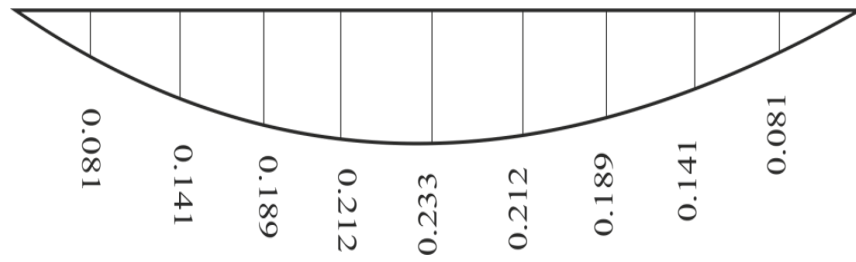
First Frequency

$$\omega_1 = 49.2 \text{ Hz}$$

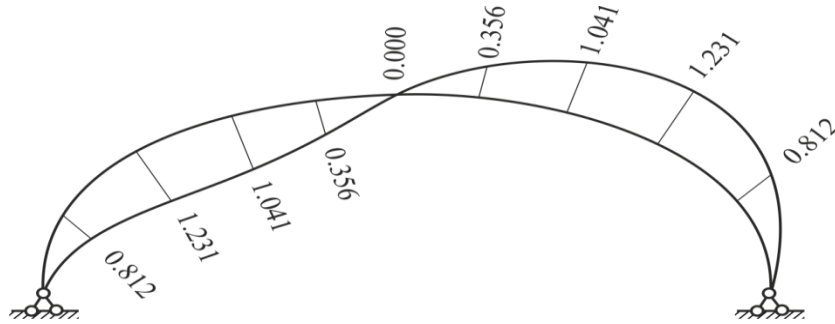
First Form of Natural Oscillations



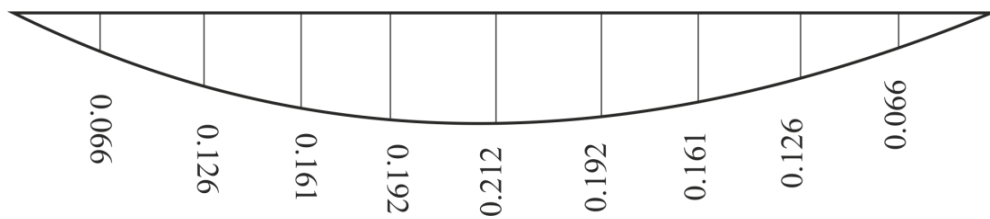
Graph 1. Amplitude values of non-dimensional movements u_3^0 in cross sections of a shell with coordinates $\alpha_1 = 0$



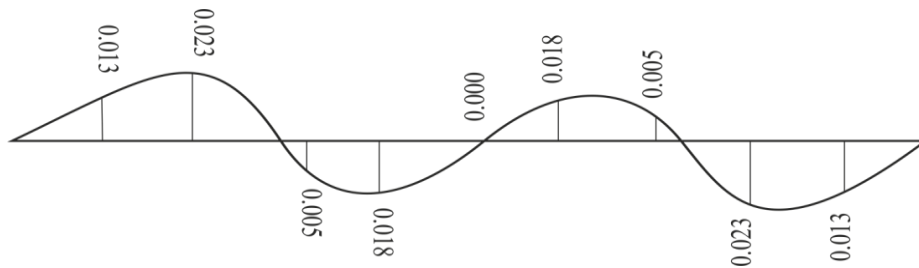
Graph 2. Amplitude values of non-dimensional movements u_2 in cross-sections of the shell with coordinates $\alpha_1 = 0$



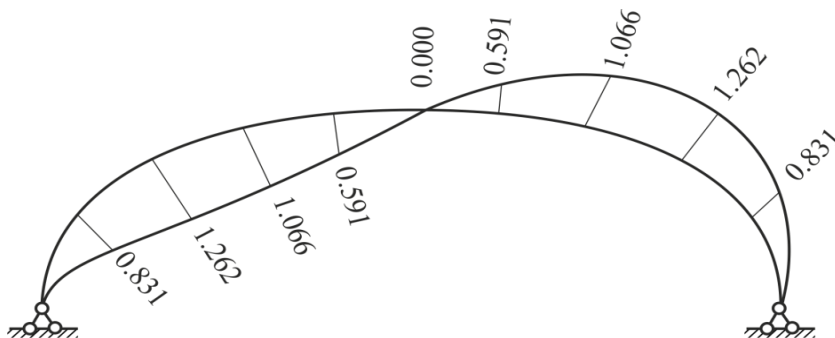
Graph 3. Amplitude values of non-dimensional movements u_3^0 in cross-sections of a shell with coordinates $\alpha_1 = \pm 0.5$



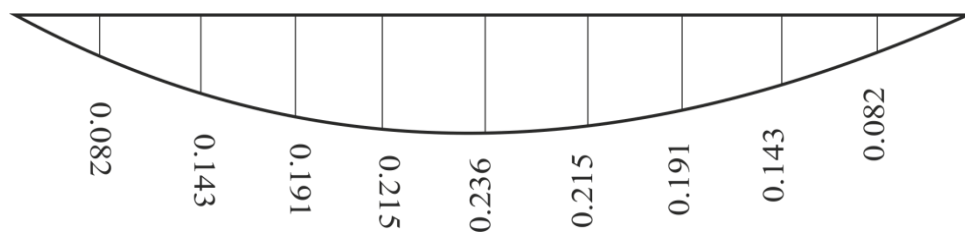
Graph 4. Amplitude values of non-dimensional movements u_2^0 in cross-sections of a shell with coordinates $\alpha_1 = \pm 0.5$



Graph 5. Amplitude values of non-dimensional movements u_1^0 in cross-sections of a shell with coordinates $\alpha_1 = \pm 0.5$



Graph 6. Amplitude values of non-dimensional movements u_1^0 in cross-sections of a shell with coordinates $\alpha_1 = \pm 0.5$



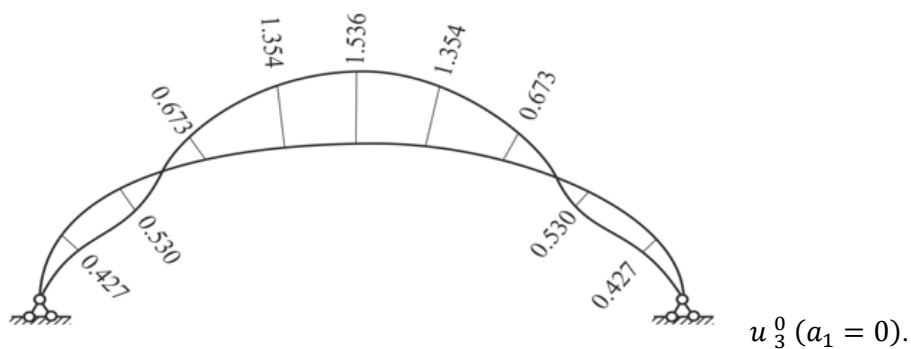
Graph 7. Amplitude values of non-dimensional movements u_2 in cross-sections of a shell with coordinates $\alpha_1 = \pm 1$

Amplitude values of non-dimensional movements u_1^0 in sections of a shell with coordinates $\alpha_1 = 0$ and $\alpha_1 = \pm 1$ are equal to zero.

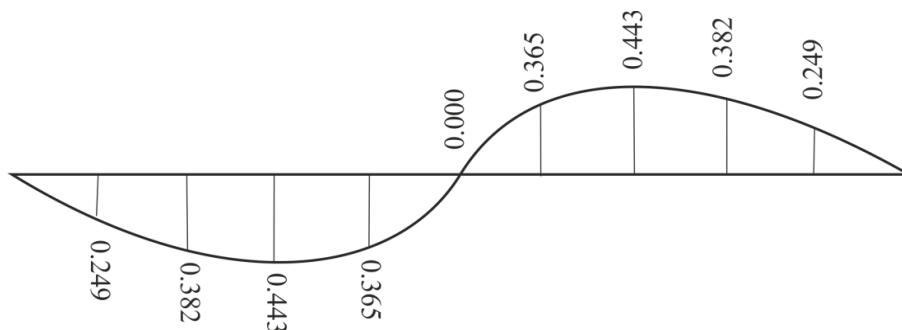
Second part

$$\omega_2 = 58.4 \text{ Hz.}$$

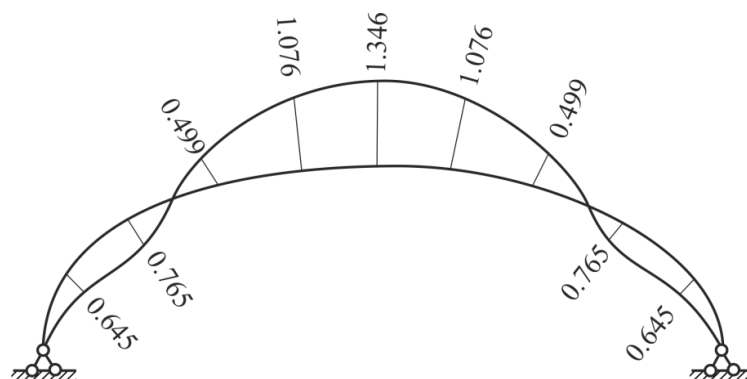
Second Form of Natural Oscillations



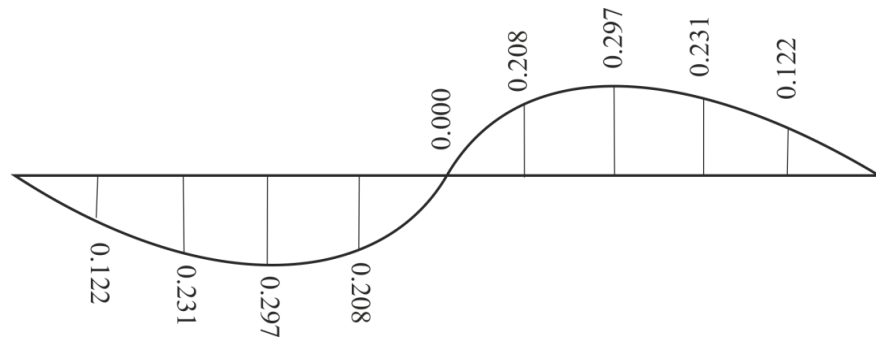
Graph 8. Amplitude values of non-dimensional movements u_3^0 in cross-sections of a shell with coordinates $\alpha_1 = 0$.



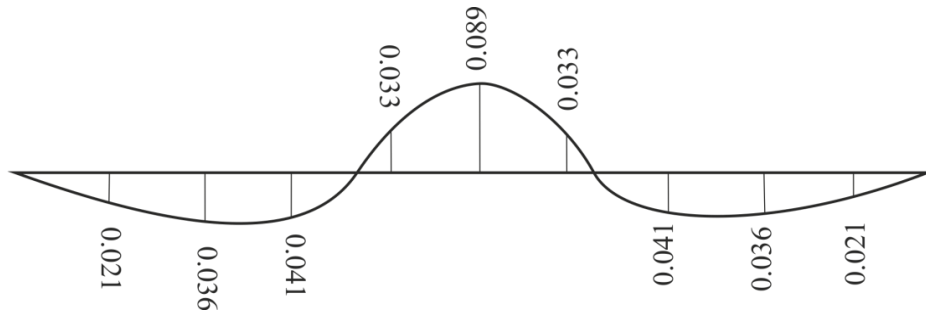
Graph 9. Amplitude values of non-dimensional movements u_2 in cross-sections of a shell with coordinates $\alpha_1 = 0$



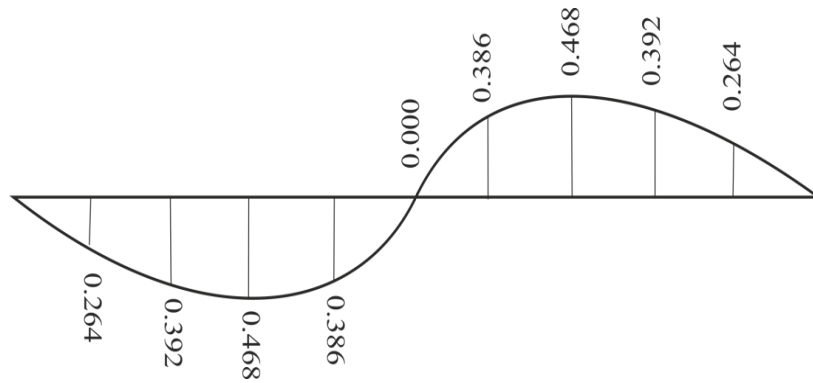
Graph 10. Amplitude values of non-dimensional movements u_3^0 in cross-sections of a shell with coordinates $\alpha_1 = \pm 0.5$



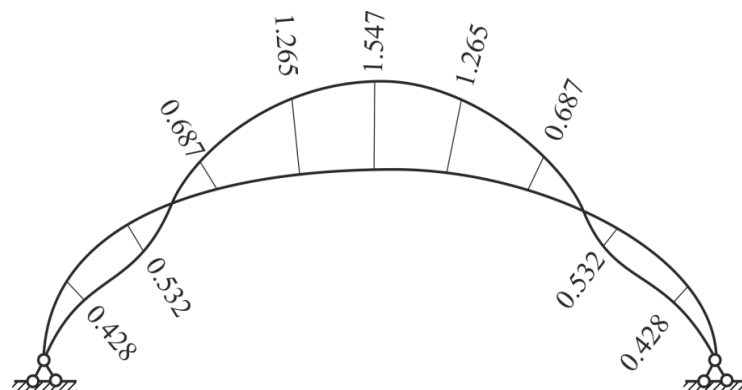
Graph 11. Amplitude values of non-dimensional movements u_2^0 in cross- sections of a shell with coordinates $\alpha_1 = \pm 0.5$



Graph 12. Amplitude values of non-dimensional movements u_1^0 in cross- sections of a shell with coordinates $\alpha_1 = 0.5$



Graph 13. Amplitude values of non-dimensional movements u_2 in cross - sections of a shell with coordinates $\alpha_1 = \pm 1$



Graph 14. Amplitude values of non-dimensional movements u_3^0 in cross - sections of a shell with coordinates $\alpha_1 = \pm 1$

Amplitude values of non-dimensional movements u_1^0 in cross-section of the shell with coordinates $\alpha_1 = 0$ and $\alpha_1 = \pm 1$ are equal to zero.

On this graphs ω_1, ω_2 are the frequencies of natural oscillations of thin wavy shells, u_1^0, u_2^0, u_3^0 are the amplitudes of non-dimensional movements of the points of shell median surface along the axes of coordinate α_1, α_2 and α_3 accordingly.

Conclusion

Analyzing the obtained values of the first three frequencies of natural oscillations of the thin wavy shell with hinge-fixed attachment of the shell along the lower contour along the generatrix, it can be noted that in this case also the fifth approach (36 members of the row) with sufficient engineering accuracy allows determining the values of the lowest frequencies. The difference between the fourth and fifth approximations by the first frequency is 2.2%, by the second is 3.4%, by the third is 4.0%. The obtained values of the lowest frequencies of the natural oscillations of the given thin wavy shell confirm good convergence of the algorithm in this case as well.

Comparison of the obtained results of calculation of these wavy shells for two options of its fixation with the rigidly caught lower contour [11] and hinge-fixed attachments shows that in the case of hinge-fixed attachment of the shell its lowest frequencies of natural oscillations have decreased by 10-16%.

In both cases, two transverse half-waves correspond to the main tone of the natural oscillations thin wavy shell.

The results of numerical calculation of this shell allow recommending the application of the proposed methodology for determination of the lowest frequencies and forms of natural oscillations of shells of complex form corresponding to them.

References

- [1]. L.V. Kantorovich, V.I. Krylov, *Priblijonnye metody vysshego analiza*. Fizmatgiz, Moscow, 1962 (in Russian).
- [2]. A.L. Goldenveiser, *Teoriya uprugikh tonkikh obolochek*. Nauka, Moscow, 1976 (in Russian).
- [3]. K.B. Aksentjan, V.D. Eryomin, *Printsip vosmojnykh peremesceniy v sluchae svobodnykh kolebaniy. Raschjot obolochek i plastin*, 1977 (in Russian).
- [4]. K.B. Aksentjan, V.K. Gordeev – Gavrikov, *Variatsionno – energeticheskiy metod raschjota kolebaniy inzenernykh sooruzheniy*. RGU, Rostov – on – Don, 1979 (in Russian).
- [5]. V.D. Eryomin, *Opreделение chastot i form sobstvennykh kolebaniy obolochek neklassicheskoy formy*. Scientific papers of National University of Architecture and Construction of Armenia, 1, 2015, 94-100 (in Russian).
- [6]. V.D. Eryomin, *Sobstvennye kolebaniya nekrugovoy cilindricheskoy uprugoy volnistoy obolochki otkrytogo profilja*. Scientific papers of National University of Architecture and Construction of Armenia, 1, 2015, 101-108 (in Russian).
- [7]. V.D. Eryomin, *K raschyotu sobstvennykh kolebaniy tonkoy volnistoy obolochki otkrytogo profilja*. Scientific papers of National University of Architecture and Construction of Armenia, 1, 2016, 64-71 (in Russian).
- [8]. V.D. Eryomin, *Issledovanie chislennoy skhodimosti algoritma opredeleniya nisshikh chastot i form sobstvennykh kolebaniy obolochek uslojnyonnoy formy*. Scientific papers of National University of Architecture and Construction of Armenia, 1, 2016, 72-77 (in Russian).
- [9]. V.D. Eryomin, *K voprosu ob issledovanii chislennoy skhodimosti algoritma opredeleniya nisshikh chastot i form sobstvennykh kolebaniy obolochek uslojnyonnoy formy*. Scientific papers of National University of Architecture and Construction of Armenia, 3, 2017, 50-55 (in Russian).
- [10]. V. D. Eryomin, *The Study of Natural Oscillations of Thin Elastic Shells of Complicated Shapes by the Energy Method*. Materials Science Forum, 931, 2018, 42-46.

- [11]. V.D. Eryomin, Opredelenie chastot i form sobstvennykh kolebaniy tonkoy uprugoy volnistoy obolochki otkrytogo profilja. Scientific papers of National University of Architecture and Construction of Armenia, 1, 2019, 26-34 (in Russian).
- [12]. V.D. Eryomin, K voprosu opredeleniya nishshikh chastot i form sobstvennykh kolebaniy tonkoy volnistoy obolochki otkrytogo profilja. Scientific papers of National University of Architecture and Construction of Armenia, 4, 2019, 20-26 (in Russian).

Victor Dmitriy Eryomin, doctor of philosophy (PhD) in engineering, professor (RF, Rostov-on-Don) - Don State Technical University (DSTU), professor at the Chair of Strength of Materials, eremin.vd@yandex.ru

Submitted: 11.01.2021

Revised: 04.02.2021

Accepted: 11.02.2021

UDC 528.5

DOI: 10.54338/27382656-2021.1-5

Yeghisabet Hakob Hayrapetyan^{1*}, Stepan Karen Petrosyan²

¹*National University of Architecture and Construction of Armenia, Yerevan, RA*

²*“VOLIOS” LLC Design Institute*

CONSTRUCTION FEATURES OF THE HIGH-PRECISION LASER RANGEFINDER LIGHT MODULATOR

The issues related to the development of a light modulator operating on the electro-optical effect of laser rangefinders by the modulation method are considered. To reduce the modulation power, it is proposed to lower the modulation frequency to 750-800 MHz, while simultaneously increasing the modulation quality to $Q = 1000$. The study of the phase determination error of a high-precision laser rangefinder depending on temperature showed that it is rational to construct the light modulator by radial installation of the KDP electro-optical crystal, with separated modulation and demodulation channels, while on combined resonators.

Keywords: *Modulation power, modulator quality, longitudinal and transverse electro-optical effects, coaxial resonator.*

Introduction

The use of optical radiation for distance measurement has long been known, and the first high-precision measurements were implemented by the interference method. The development of laser technology has further enhanced the role of interference measurement method. However, interference measurements are extremely laborious, are difficult technically and organizationally and require detailed preliminary works [1]. Therefore, such measurements are still used for solving special issues. It should also be noted that the certification and operation of an interferometer is a complex technical issue.

This has led to using other methods to perform high-precision linear measurements. The modulation method has become the primary method for high-precision linear measurements and the light modulators in high-precision laser rangefinders operate on the linear electro-optical effect [2]. In this regard, the study of the specificity of modulator operation and the discovery of ways to effectively use light modulators constructed on KDP electro-optical crystal allows wider application of laser rangefinders in various fields of science and technology.

Further development of UHF (ultra-high frequency) rangefinders is related not only to the development of new measurement principles and methods, but also the improvement of different units of light rangefinders, which will allow to implement the potential opportunities of this or that method. For the construction of a high-precision light rangefinder with measurement error in the range of $(0.05 \dots 0.2) \text{ mm}$, it is necessary to solve several problems, the main of which are the choice of optical radiation modulation and phase-detection methods.

Main Part

After certification and testing of CD-1200 model [4] modernized on the basis of the DVCD-1200 [3] laser rangefinder, a number of questions arose, which are considered in the present paper.

Multiple measurements taken at different comparators aimed at the determination of the device phase - m_k and device constant - m_k errors, showed that for compensation rangefinder $m_{\varphi} = m_k = 0.07 \text{ mm}$ was obtained. It was also confirmed that to implement biphasic mode of the modulation method, the potential accuracy of the phase measurement may be $m_{\varphi} = 0.01 \dots 0.03 \text{ mm}$ and such device is capable of self-certification.

All this shows the possibility to build a reference rangefinder, which is necessary for studying the movements of the Earth's crust and controlling the length of national bases and comparators. It is possible to build a reference rangefinder under the following conditions:

- Reduction of modulation power, to decrease the heating of the light modulator-demodulator (modem) crystal, which causes phase emissions in frontal part of the modulated light, installation of receiver optics which not only increases the intensity of light coming from the area, but also averages the modular phase emissions.
- It is necessary to exclude the imposition of a transverse electro-optical effect (EOE) to longitudinal electro-optical effect in the electro-optical KDP crystal during the modulation-demodulation process, which is caused by the curvature of the electric field lines passing through the crystal. The longitudinal electro-optical effect takes place when the direction of light propagation coincides with the direction of the electric field, and the transverse electro-optical effect happens when their directions are perpendicular to each other.
- To maintain the optimum parameters of the dimensional resonator of light modem with a KDP crystal, the scale frequency UHF auto generator should not be combined with the light modem in the same resonator.

Consider the peculiarities of the above-mentioned conditions, focusing primarily on the reduction of modulation power, using the well-known expression [5]

$$P_m = \frac{U^2 \cdot C_m}{2} = \frac{U^2 \cdot \omega_m c_m t g \delta}{2} = \frac{U^2 \cdot \omega_m c_m}{2Q_m}, \quad (1)$$

where U is the voltage applied on the crystal, Q is the modulation quality, c is the capacity, $\omega = 2\pi f$, where f is the modulation frequency.

Q_m is presented as the result of the parallel connection of an electro-optical crystal Q_{kp} and resonator Q_p

$$Q_m = \frac{Q_{kp} \cdot Q_p}{Q_{kp} + Q_p}.$$

During the calculation of the light modulator, the output data is the modulation frequency, the reduction of which leads to a significant decrease in the modulation power. At the same time, the phase determination error is conditioned by the magnitude of the modulation frequency with the following regularity: $m_\phi = (10^{-3} \dots 10^{-4})\lambda$, according to which an increase in frequency leads to the decrease of phase determination error.

The problem solution can be provided with the application of a new biphasic modulation method, in which two signals deviated from each other by 180° are generated optically and the position of the equality of their amplitudes is recorded. That is, the record of the measurement result is implemented in the average linear area of the demodulation characteristics (the dependence of the relative intensity of light coming from the area on distance). In this case, the phase determination error - m_ϕ is significantly reduced and there is an opportunity to reduce the frequency f . At this stage, the application of the biphasic method allows to reduce the frequency from 1200 MHz to 800... 1000 MHz [6,7].

According to [3], the voltage U on the light modulator crystals in case of low powers can be provided under the conditions of high quality Q modulator.

At frequencies below 800 MHz, the coaxial resonator sizes are considerably larger, which reduces the quality of the light modulator. At high frequencies (1200 MHz and more) the resonance resistance of the modulator decreases due to losses in the electro-optical crystal and the quality is in the range of $Q = 800$. At 800... 1000 MHz frequencies the sizes of the resonator are not large and the modulator quality is within the limit of half of the KDP crystal ($Q_{KDP} = 2000$) quality, $Q = 1000$.

In a coaxial resonator, according to Fig. 1, depending on the D/d ratio, there is a certain gap size Δ where the KDP crystal is placed, in case of which the electric power lines of the TEM field reach the end of the

resonator without curving. The Δ gap size is equal to crystal length ℓ_{kp} , and is determined from the condition of the crystal optimal length $\ell_{kp_{opt}} = \lambda_M / 5.5n_0$.

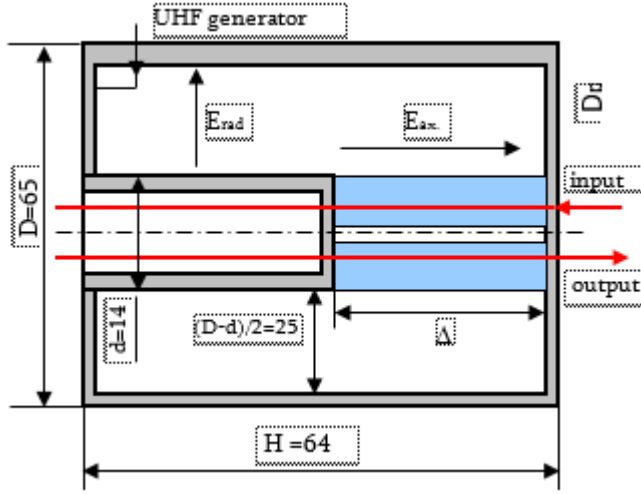


Fig. 1. The main dimensions of the coaxial resonator

for the modem in Fig. 2., where $\lambda/4 = 250 \text{ mm}$ ($f_m = 1200 \text{ MHz}$). In the DVCD -1200 modulator, a 35 mm electro-optical KDP crystal placed in a $\Delta = 35 \text{ mm}$ gap, which is 10 mm larger than the $(D-d)/2$ gap.

This results in the simultaneous operation of longitudinal and transverse electro-optical effects. The presence of a longitudinal electro-optical effect leads to an increase in the thermal dependence of the light modulation phase, which causes phase emissions in the frontal part of the modulated light. This is one of the main reasons for the high value of phase determination error - $m_\varphi = 0.25 \dots 0.3$ of the DVCD -1200 rangefinder.

The nature of the distribution of power lines of the electric field E in a coaxial resonator is also confirmed by a photo taken by a thermal imager (Fig. 3) at the Scientific Research Institute in Kharkov (Ukraine), which shows the distribution of the thermal field in the crystal. The difference in temperature along the 35 mm electro-optical crystal is $T_1 - T_3 = 6^\circ\text{C}$, which is the reason for the spread of the modulation phase of $\pm 0.25 \text{ mm}$ in the cross section of the modulated light.

This photo proves that the power lines of the E_{ax} field do not reach the end of the resonator, i.e. the E field is not applied along the entire length of the crystal. In addition, E field is applied in both axial and radial directions. Although the calculation efficiency of the modulation is preserved, according to which the optimal length of the crystal is determined, a part of the modulation efficiency is formed by the transverse electro-optical effect, which is not desirable in phase measurements. To implement only a longitudinal electro-optical effect in the light modulator, it is necessary to place it in the resonator in the radial direction, because distortion of the power lines of E_{rad} electric field does not occur in this direction, reducing the crystal length (Fig. 2). Thus, the crystal length on the longitudinal

However, the concept of the optimal length of the crystal should not be used for obtaining longitudinal electro-optical effect, but the nature of the E electric field power lines should be taken into account.

The E field power lines in Δ gap are closed on the resonator cylinder, as shown in Fig. 2 (the given dimensions correspond to the DVCD-1200 light modem). In this case, for a coaxial resonator, starting from the $\Delta \geq \frac{D-d}{2}$ condition, the expected decrease in length H from $\lambda/4$ does not depend on the Δ gap size and the $\lambda/4$ length of the resonator can be equal or greater than as

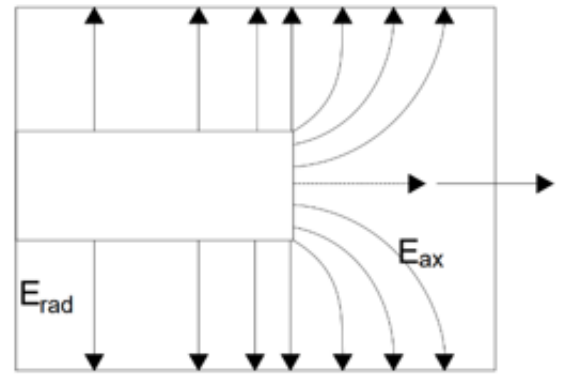


Fig. 2. The image of E field, when $\Delta > (D - d) / 2$

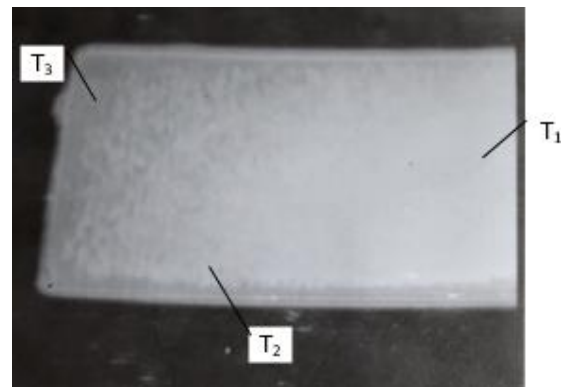


Fig. 3. Thermal field distribution in the crystal

electro-optical effect must be determined taking into account the minimum losses of the light modulator, which is primarily conditioned by the D/d ratio of the resonator for the selected modulation frequency.

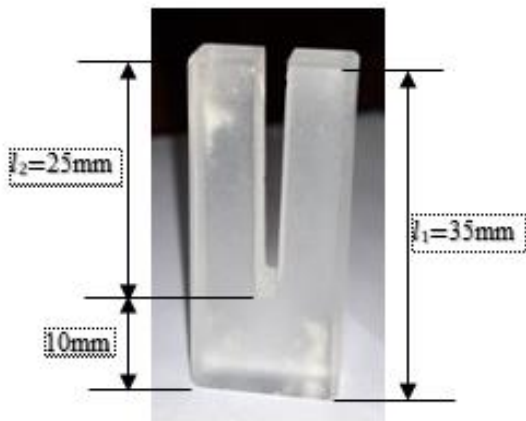


Fig. 4. KDP crystal form

the laser beam passes through the crystal is completely excluded. The groove length l_2 is related to the l_1 crystal length with the following ratio $l_2/l_1 = 0.7 \dots 0.8$.

Although 5... 7% modulation efficiency loss takes place in the crystal, the phase error decreases to the value $m_\varphi = 0.07 \text{ mm}$. The study of this issue showed that the size of the coaxial resonator gap Δ should be determined according to the Δ/D curve presented in Fig. 5 [5].

For the resonator shown in Fig. 1, $D/d \approx 4.7$, or $d/D = 0.215$ and respectively $\Delta/D = 0.15$ or $\Delta = 0.15 \cdot 65 = 10 \text{ mm}$. In this case, the capacity of the gap, according to the curve shown in Fig. 5 will be

$$C_\Delta = FD = 0.05 \cdot 6.5 = 0.325 \text{ pF}.$$

Since in coaxial resonators the direction of the power lines of E_{rad} electric field does not depend on the size of the gap Δ and according to the magnitude of the voltage the radial and axial components of the electric field E are equal to each other - $E_{rad} = E_{ax}$, and the concentration of the power lines in the axial direction is higher, for light modulation-demodulation it is rational to place the crystals radially, because in case of the same modulation efficiency the radial crystal heats up less, i.e. it consumes less UHF power than in the case of axial installation of a KDP electro-optical crystal. If the modulation efficiencies are equal in case of axial and radial installations of the crystals during the experimental measurements, it will be possible for the high-precision rangefinder to build a light modulator with separated modulation and demodulation channels on connected resonators, which will allow to connect the transmitter-receiver optics directly to the light modem. The length of the radially installed crystal should be determined from the condition of the optimal resonator capacity, the size of which for the given gap is determined by the curves shown in Fig. 5.

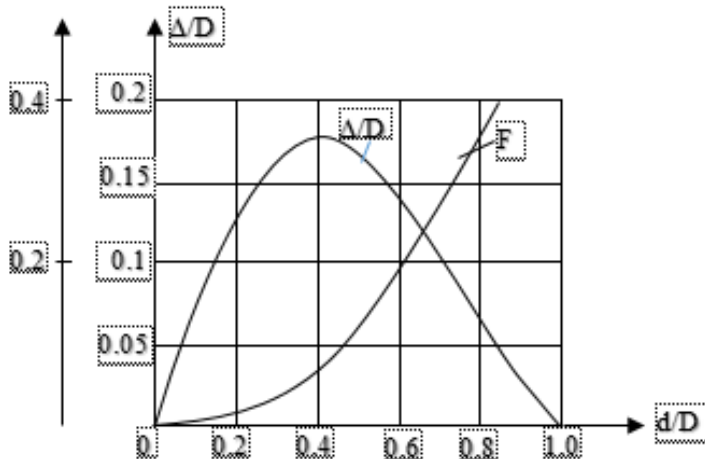


Fig. 5. Curves for modulator calculation

Taking into account the fact, that less heating of the crystal reduces the phase emissions of the light received from the area to the front part, a 35 mm long crystal with a groove was used in the CD-1200 light rangefinder, Fig. 4 [9]. The implementation of the longitudinal groove along the crystal center allows to form receiver-transmitter channels in the crystal, at the same time maintaining the uniformity of light modulation and demodulation, by separating modulation-demodulation channels optically, as a result of which the penetration of internal reflections from the crystal output front into the analyzer exit as

Focus on the issues of the light modulator structure. The first results of the light modulator study led to the conclusion that by dividing the resonator into 2 parts, where the gaps are proportional to the half of the crystal length $\frac{l_{kp}}{2}$, it is possible to combine 2 resonators with radially installed crystals. We will get a light modem with split channels of modulation and demodulation (Fig. 6) on the combined resonators. To excite the modulator, a

large-scale UHF generator can be connected to the "aa" attachment line. The peculiarity of the two-side coaxial resonator is that the modulator can be excited in 2 modes – synchronous and antiphase. A strong electric field in the gap of the resonator allows to carry out modulation frequency addition in a significant range by introducing V volume dielectric. The distance D_{avr} between electro-optical crystals is $D_{avr} = 30 \text{ mm}$, which is the average diameter of the receiver-transmitter optics.

Estimate the modulation power reduction for the new modulator. For a KDP crystal when the light wavelength is $\lambda = 0,6328 \mu\text{m}$, the half-wave

voltage is $U_{\lambda/2} = \frac{\lambda}{2n_0^3 r_{63}}$ [10], where n_0 is the refractive index of the KDP crystal for a regular wave and $n_0 = 1.47$, r_{63} is the electro-optical coefficient, $r_{63} = 10.5 \cdot 10^{-10} \text{ cm/V}$, which results in $U_{\lambda/2} = 9500 \text{ V}$. According to the expression (1), the $P_{\pi \text{ calc.}}$ calculation half-wave power for a frequency of 1200 MHz will be:

$$P_{\pi \text{ calc.}} = \frac{(9500)^2 \cdot 2 \cdot 3,14 \cdot 12 \cdot 10^8 \cdot 0,95 \cdot 10^{-12}}{2 \cdot 800} = 410 \text{ W}.$$

The ratio $\frac{I}{I_0}$ of modulated and demodulated light intensities is determined experimentally in the case of P_m of certain modulation powers. Then from the equation $\frac{I}{I_0 = 0,5 \left[1 - J_0 \left(\sqrt{\frac{P_m}{P_{\pi}}} \right) \right]}$ the value of $P_{\pi \text{ exp.}} = 450 \text{ W}$ is determined. The difference in powers $P_{\pi \text{ exp.}} - P_{\pi \text{ calc.}} = 40 \text{ W}$ is due to losses of stable wave coefficient.

Among the well-known solutions that reduce the light rangefinder modulation power, let us point out the biphasic mode of accurate linear measurement, where the optimal ratio $U/U_{\pi} = 0.54$ takes place and the modulation power at the $P_{m\varphi} 1200 \text{ MHz}$ frequency is $P_{m\varphi} = (0.54)^2 \cdot P_{\pi \text{ ex.}} = 131 \text{ W}$.

If the modulation frequency is reduced to 800 MHz , i.e., electro-optical crystal capacity is reduced by 1.5 times and the modulator quality is raised to $Q = 1000$, the magnitude of the half-wave power will be:

$$P_{\pi \text{ calc.}} = \frac{(950)^2 \cdot 2 \cdot 3,14 \cdot 8 \cdot 10^8 \cdot 0,65 \cdot 10^{-12}}{2 \cdot 1000} = 150 \text{ W}.$$

Taking into account the losses, we can assume that $P_{\pi} = 180 \text{ W}$. Since $P_m = P_{\pi} \cdot \left(\frac{U}{U_{\pi}} \right)^2$, in compensation mode it will be $P_m = 180 \cdot (0.61)^2 = 67 \text{ W}$. In the biphasic operation mode we will have:

$$P_m = 180 \cdot (0.54)^2 = 53 \text{ W}.$$

Conclusion

Thus, the construction scheme of a high-precision light rangefinder should be based on light modulation-demodulation in biphasic mode, and the electro-optical crystal KDP should be placed in the radial direction in the resonator excited by the TEM wave.

As a result of studies, a new type of light modulator is proposed, which will allow to create a high-precision laser rangefinder, providing a phase error of $m_{\varphi} = 0.03 \dots 0.05 \text{ mm}$. If modulators with axial and radial installation of crystals have equal modulation efficiency, it is rational to build the light modem for laser rangefinder on resonators combined with separated modulation-demodulation channels, which will allow to directly connect the receiver-transmitter optics with the light modem.

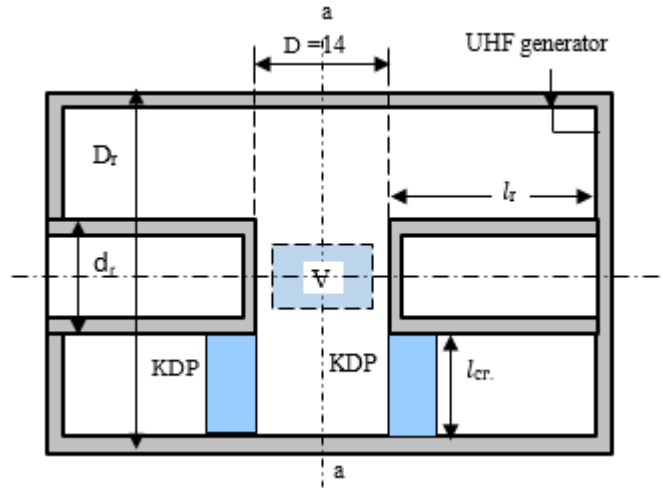


Fig. 6. Light modem with separate light modulation-demodulation channels

In a high-precision light rangefinder, it is preferable to perform laser light modulation-demodulation on the electro-optical effect in the frequency range of 750... 800 MHz, increasing the modulator quality up to $Q = 1000$, which will allow to significantly reduce the modulation power.

The study of the temperature-dependent phase error showed that the size of the coaxial resonator Δ gap should be determined according to the curves shown in Fig. 5.

References

- [1]. V.D. Bolshakov, F.Deymlikh, A.N. Golubev, V.P. Vasilyev, Radio-geodetic and electro-optical measurements. Nedra, Moscow, 1985 (in Russian).
- [2]. H. Kamen, Electronic measurement methods in geodesy. Nedra, Moscow, 1982.
- [3]. A.G. Beglaryan, K. S. Gyunashyan, Ye.H. Hayrapetyan, High precision light range-finder DVCD-1200 for linear comparator. Proceedings of 3rd international conference on contemporary problems of architecture and construction, Beijing, China, Nov. 20-24, 2011, 5-8.
- [4]. K.S. Gyunashyan, R.R. Sinanyan, Ye.H. Hayrapetyan, Constant "K" of the CD-1200 light range finder and the results of production tests. Geodesy and aerial photography, 4, 1996, 136-143.
- [5]. H. Meinke, F. Gundlakh, Radio-technical reference book. Gosenergoizdat, Leningrad, 1, 1960.
- [6]. Ye.H. Hayrapetyan, H.S. Petosyan, H.A. Hunanyan, A.S. Tsaturyan, High-precision two-phase laser rangefinder PFSD-1,2 international scientific conference on construction the formation of living environment 2019 (FORM 2019), Tashkent, April 18-21, 2019, 1-9.
- [7]. K.S. Gyunashyan, E.A. Hayrapetyan, Phase light range finder, RR Patent 1598613 (1990).
- [8]. E.A. Hayrapetyan, S.K. Petrosyan, V.G. Harutyunyan, A.A. Khachatryan, Vybor modulyatora sveta etalonnoy svetodal'nomera. Bulletin of National University of Architecture and Construction of Armenia, 1, 2020, 50-57 (in Russian).
- [9]. K.S. Gunashyan, E.A. Hayrapetyan, V.G. Harytunyan, Kh.V. Vardanyan, Microwave modulator-light demodulator, RR patent 1420367 (1988).
- [10]. E.R. Mustel, V.N. Parygin, Methods of modulation and scanning of light. Nedra, Moscow, 1970.

Yegisabet Hakob Hayrapetyan, *doctor of philosophy (PhD) in engineering, associate professor (RA, Yerevan) - National University of Architecture and Construction of Armenia, senior scientist at the Problem Laboratory of Geodetic Measurements, helizabet@yandex.ru*

Stepan Karen Petrosyan (RA, Yerevan) - "VOLIOS" LLC Design Institute, engineer, styop.petrosyan96@mail.ru

Submitted: 06.05.2021

Revised: 10.05.2021

Accepted: 17.05.2021

Marine Ashot Kalantaryan^{1*}, Avetik Artavazd Arzumanyan¹

¹ National University of Architecture and Construction of Armenia, Yerevan, RA

WATER ABSORPTION CAPACITY OF IRIND MINE PUMICE

Water absorption capacity of Irind mine pumice depending on the particle size and absorption time is presented in the paper. Irind pumice is an aluminosilicate rock, with well-developed porosity, mechanical strength, high buoyancy, chemically inert, eco-friendly and exhibits sufficient water absorption capacities. The examination of the pumice by X-ray diffractometry has shown that it is a volcanic rock and is composed of cristobalite and coesite. The following particle sizes were selected for the study: 1.5... 2.0 mm, 2.5 ... 5.0 mm. Water absorption capacity of pumice was determined depending on the absorption period. The maximum water absorption was observed for particle sizes ranging from 2.5 to 5.0 mm.

Keywords: absorbent, pumice, water absorption, particle sizes, porosity.

Introduction

Water pollution is becoming a major concern, because of the increasing numbers and concentrations of persistent and toxic anthropogenic pollutants in water resources. Many recent studies have considered new absorbents to remove these emerging contaminants from water resources.

There are number of water purification methods, but the adsorption is the simplest and effective. The development of low-cost absorbents has led to the rapid growth of research interests in this field. Many absorbents based on natural and waste materials and requiring minimal processing have been proposed. In this article solid absorbents such as Irind pumice has been discussed. Pumice is a type of extrusive volcanic rock, produced when lava with a very high content of water and gases is discharged from a volcano. As the gas bubbles escape, the lava becomes frothy. When this lava cools and hardens, the result is a very light rock material filled with tiny bubbles of gas. Commonly it is light-colored, indicating that it is a volcanic rock high in silica content.

The Republic of Armenia takes a lead in the world with abundance and diversity of non-metallic minerals. Nearly all types of mineral rocks well known all over the world exist in the territory of the country. Mountainous rocks formed as a result of volcanic processes in the territory of Armenia are of special value and significance, the most important of which are light rocks (tuffs, perlite, pumice-stone, zeolite, scoria, etc.). In this article the properties of Irind mine pumice is considered (Fig. 1).



Fig. 1. Sizes of Irind mine pumice grains. a) 1.5 to 2.0 mm, b) 2.5 to 5.0 mm

Irind is located in Talin region. It is 46 km away from the regional center. There are perlite and pumice resources in the village, which are of industrial importance. In the Republic of Armenia pumices according to their physical-mechanical characteristics are divided into two types: Ani type and lithoid pumices.

The Irind mine pumice is one of the Ani type varieties. Ani-type pumice is mainly composed of glass non-crystalline (amorphous) particles: plagioclase, pyroxene and mineral crystals, pieces of old lava. The color is yellowish, somewhere yellow-brown, pink-yellow, the porosity is 35...44%. It has quite high thermal insulation properties. The bulk density of the pumice is 0.3...0.6 g/cm³ [1,2].

Chemical composition of Irind pumice is presented in Table 1 [1].

Table 1. Chemical composition of Irind pumice, %

Region	SiO ₂	MgO	TiO ₂	Fe ₂ O ₃	K ₂ O + Na ₂ O	Al ₂ O ₃	SO ₃	CaO	loss on Ignition
Irind mine pumice	61.54	1.13	0.43...1.00	3.99...4.99	8.18	16.58...17.49	-	3.78... 4.20	2.37

In Table 2 physical and mechanical properties of Irind mine pumice is presented.

Table 2. Physical and mechanical properties of Irind mine pumice

N	Bulk density, g/cm ³	Specific weight, g/m ³	Porosity, %	Tensile strength, kg/cm ²
Irind mine pumice	382...749	2.43...2.46	69.3...84.3	14...19

The examination of the pumice by X-ray diffractometry have shown that it is a volcanic rock and is composed of cristobalite and coesite (Fig. 2).

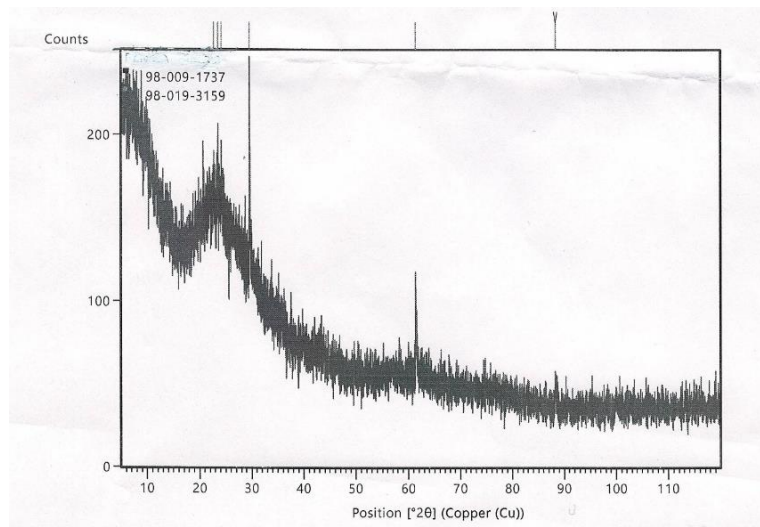


Fig. 2. X-ray diffraction analysis

Coesite and cristobalite are high-pressure polymorph (crystal form) of silica, silicon dioxide (SiO₂). They have the same composition but possess a different crystal structure.

In Table 3 the crystal structure of pumice is presented.

Table 3. Identified Patterns List

Visible	Ref. code	Score	Compound name	Displ. [°2θ]	Scale fac.	Chem. formula
*	98...009-1737	20	Cristobalite	0.222	0.498	SiO ₂
*	98...019-3159	26	Coesite	- 0.217	0.630	SiO ₂

The presented data show that Irind mine pumice is an aluminosilicate rock, with well-developed porosity, mechanical strength, high buoyancy, chemically inert and eco-friendly. Due to the above mentioned properties, the Irind pumice can be used as an oil absorbent, therefore it must exhibit certain water - and oil absorption capacities [3].

In this article the water absorption capacity of pumice is observed. Particles with sizes 1.5... 2.0 mm and 2.5...5.0 mm were selected for the study. In the beaker filling with 50 ml of the absorbate (oil and water) were put about 2 grams of the absorbents. The sorption process was calculated after 1, 2, 3, 5, 8, 10, 15, 20, 30, 60, 90, 120 minutes of the sorption time [3] and the absorbed amount of water was detected. The maximum water absorption was detected by particles with sizes ranging from 2.5 to 5.0 mm. The obtained water absorption values clearly suggest that the pores can be saturated with water under standard barometric pressure [4]*.

Fig. 3 shows the water absorption capacities of two different particles.

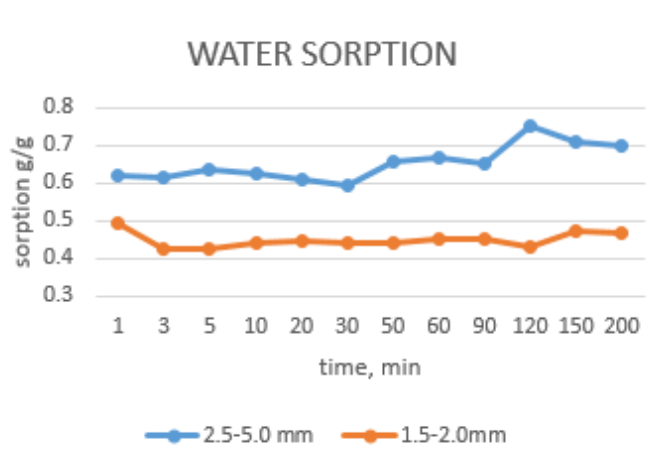


Fig. 3. Water absorption capacity of 1.5...2.0 mm and 2.5...5.0 mm particles

Conclusion

Studies have shown that the pumice has improved porosity and exhibits sufficient water absorption capacities. The results of the experimental runs for the adsorption of water on Irind pumice of two particle sizes are thus presented. The amount adsorbed on 2.5 ... 5.0 mm particles was the highest, followed by 1.5...2.0 mm particles.

Water absorption has been studied for 2 hours. It can be seen from the graph that the maximum water absorption capacity is observed for 2.5...5.0 mm particles, which is 0.75 g/g after 2 hours. It is planned to carry out sorbent oil absorption capacities and sorbent surface modification in order to decrease water sorption and increase oil sorption capacities.

References

- [1]. Z.A. Hacagortsyan, Prirodnie kamennie materiaali Armenii. SSSR. Stroiizdat, Moscow, 1967 (in Russian).
- [2]. Gornaya entsiklopediya. Sovetskaya entsiklopediya. Pod redaktsiey Ye.A. Kozlovskogo, Moscow, 1984-1991 (in Russian).
- [3]. Y. D. T Trang, L. A. Zenitova. Study on the sorption capacity of the adsorbent based on polyurethane and chitin to remove oil spills. IOP Conference Series: Earth and Environmental Science, vol. 337, Efficient waste treatment, 13–14 December, 2018.
- [4]. J. McPhie, M. Doyle, R. Allen, Volcanic Textures: a guide to the interpretation of textures in volcanic rocks. Centre for Ore Deposit and Exploration Studies, University of Tasmania, Hobart, Tasmania, 1993.

* GOST 8269.0-97 Crushed stone and gravel made from dense rocks and industrial waste products for construction works. Methods of physical and mechanical tests.

Marine Ashot Kalantaryan, doctor of philosophy (Ph.D) in chemistry (RA, Yerevan) - National University of Architecture and Construction of Armenia, assistant at the Chair of Production of Construction Materials, Products and Structures, kalantaryanm@mail.ru

Avetik Artavazd Arzumanyan, doctor of philosophy (PhD) in engineering, associate professor (RA, Yerevan) - National University of Architecture and Construction of Armenia, lecturer at the Chair of Production of Construction Materials, Items and Structures, avetikarzumanyan@gmail.com

Submitted: 08.04.2021

Revised: 25.04.2021

Accepted: 02.05.2021

Khachik Arthur Shahbazyan

National Polytechnic University of Armenia, Yerevan, RA

STUDY OF METHODS FOR ASSESSING THE LEVEL OF ENERGY SECURITY AND THE WAYS TO IMPROVE

The most common methods of energy security assessment have been studied, and possible deviations of results in the condition of their application have been estimated. The ways of their improvement as a result of the implementation of these methods in the conditions of the Republic of Armenia have been identified.

Keywords: *Energy security, electricity, method, managerial influence, weight of importance.*

Introduction

As is well known, the choice of method for assessing the level of energy security (ES) has a significant impact on the accuracy of the result obtained. Examining the work related to the assessment of the level of ES by a number of international and domestic experts and specialists, one can confirm that opinion, that depending on the infrastructural features of the state, the method of security assessment can be differentiated from the results obtained at the ES level. That is why we will consider the most common methods of assessing the level of ES.

The concept of ES level zones has become widespread in the scientific community, which allows to characterize the ES level as ES - situations in normal (N), pre-crisis (PC) or crisis (C) zones [1].

Materials and methods

The ES level assessment process is based on the following basic provisions [2]:

1. If one of the ES level assessment indicators is considered to be in a crisis situation, then regardless of the status of the other indicators in the system, the ES level of the country is evaluated as critical.
2. If two ES level assessment indicators are considered to be in a pre-crisis situation, then regardless of the status of other indicators in the system, the ES level of the country is assessed as critical.
3. If one of the ES level assessment indicators is considered pre-crisis, and other indicators are assessed as being within the normal zone, then regardless of the status of other indicators, ES level of the country is assessed as pre-crisis.
4. Each indicator used for ES level assessment has a minimum value threshold for descriptive situations,
5. The more the number of indicators below the value threshold defining the crisis situation, the deeper the crisis of the country's energy system.

Research methods

The most common methods of ES level assessment are [3]:

1. Scalar method,
2. Intersecting planes method,
3. Discriminant analysis method,
4. The method of fuzzy sets.

The scalar method is based on the principle of the point assessment, the purpose of which is to assess the country's ES level and to determine the situation zone as a result of point assessments and system of ES indicators.

The application of the scalar method makes it possible to consider the multidimensional function of ES level assessment indicators as one-dimensional [4]. To classify situations describing the ES level and to include them in situational zones, a point assessment system must be applied. When carrying out indicator analysis, it

is important for the scalar indicators to have the same direction of influence on the ES level. When choosing a direction, we can consider the conditional direction of the influence, and carry out scaling of the indicators examining the direction of the unit change of the indicator on the ES level.

The schematic structure of the scalar method application for the assessment of ES level is presented in Fig.1.

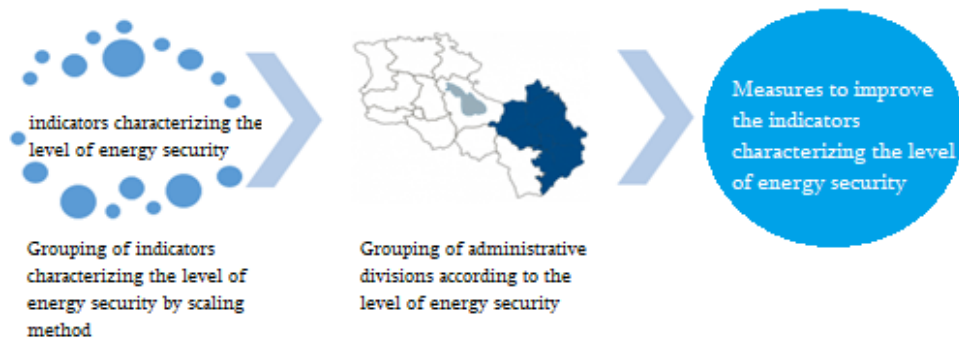


Fig. 1. Schematic Diagram of the Scalar Method Application

Using the scalar method, we can formulate a set of characteristic indicators of ES level and based on their calculation, assess the state ES level in different calculation periods.

With the aforementioned method, the following sets were formed: Electricity supply security for consumers (X1), Resource (fuel-energy) provision for the power supply system (X2), Reliability of fuel and power supply (X3), Depreciation of main production funds of the power system, provision of depreciation funds (X4), Environmental security of energy system (X5), Security of power supply and energy-efficient systems (X6), Education level for energy professionals (X7) [6].

The weight of the influence of the indicators characterizing the ES level, being in the range of $1 \leq r_{ir} \leq m$, where m and r_{ir} - are the number and order of the indicators, respectively, is important in the application of the scalar method [7].

The weight of the influence of the indicators characterizing the ES level is determined as follows:

$$C_{ir} = 1 - (m)^{-1}(r_{ir} - 1), \quad (1)$$

and the weight of the i indicator will be determined as follows:

$$B_{ir} = C_{ir} / (\sum_{i=1}^m C_{ir}), \quad (2)$$

$$B_i = (R)^{-1} \sum_{r=1}^R (C_{ir} / \sum_{i=1}^m C_{ir}): \quad (3)$$

Consider the above-mentioned indicators characterizing the country's ES level, and the application of the scalar method (Table) for 7 sets based on them.

Table. Determination of the order of importance of the indicators, characterizing the ES level for the country by scalar method

The set characterizing the ES level	Order		C_{i1}	C_{i2}	B_{i1}	B_{i2}	B_i
	1	2					
K ₁	4	3	0.57	0.71	0.142	0.178	0.16
K ₂	5	7	0.43	0.14	0.108	0.035	0.072
K ₃	3	2	0.71	0.86	0.178	0.215	0.197
K ₄	6	4	0.29	0.57	0.072	0.142	0.107
K ₅	1	1	1	1	0.25	0.25	0.25
K ₆	2	5	0.86	0.43	0.215	0.108	0.161
K ₇	7	6	0.14	0.29	0.035	0.072	0.051
\sum	-	-	4	4	1	1	1

The accuracy of the capacity calculation can be checked as follows:

$$\sum_{i=1}^n B_{ir} = 1, r=\overline{1,7}, \sum_{i=1}^n B_i = 1. \quad (4)$$

Having obtained the order of importance of the sets of indicators characterizing the ES level, the following system of equations can be formulated [8].

$$\begin{cases} \frac{dK_1}{dt} = a_{11} + a_{12}K_2(t) + a_{13}K_3(t) + a_{14}K_4(t) + a_{15}K_5(t) + a_{16}K_6(t) + a_{17}K_7(t) \\ \frac{dK_2}{dt} = a_{21}K_1(t) + a_{22} + a_{23}K_3(t) + a_{24}K_4(t) + a_{25}K_5(t) + a_{26}K_6(t) + a_{27}K_7(t) \\ \frac{dK_3}{dt} = a_{31}K_1(t) + a_{32}K_2(t) + a_{33} + a_{34}K_4(t) + a_{35}K_5(t) + a_{36}K_6(t) + a_{37}K_7(t) \\ \frac{dK_4}{dt} = a_{41}K_1(t) + a_{42}K_2(t) + a_{43}K_3(t) + a_{44} + a_{45}K_5(t) + a_{46}K_6(t) + a_{47}K_7(t) : \\ \frac{dK_5}{dt} = a_{51}K_1(t) + a_{52}K_2(t) + a_{53}K_3(t) + a_{54}K_4(t) + a_{55} + a_{56}K_6(t) + a_{57}K_7(t) \\ \frac{dK_6}{dt} = a_{61}K_1(t) + a_{62}K_2(t) + a_{63}K_3(t) + a_{64}K_4(t) + a_{65}K_5(t) + a_{66} + a_{67}K_7(t) \\ \frac{dK_7}{dt} = a_{71}K_1(t) + a_{72}K_2(t) + a_{73}K_3(t) + a_{74}K_4(t) + a_{75}K_5(t) + a_{76}K_6(t) + a_{77} \end{cases} \quad (5)$$

The system of 5 equations makes it possible to assess the ES level taking as a basis the value of the indicators characterizing the ES level and the weight of their importance.

$$ESI = \sqrt[7]{\prod_{i=1}^7 \frac{dK_i}{dt}} : \quad (6)$$

The intersecting planes method is based on indicator analysis and allows to present the obtained results through a two-dimensional plane.

As we have already mentioned, based on the calculations, the ES level is characterized by its situational zones, according to which we will have 3 zones of ES on two-dimensional planes for situations N, PC and C, respectively.

In plane building process, we are guided by the baselines underlying the ES level assessment.

Consider the two-dimensional image of ES level assessment with the method of intersecting planes $R^2 = \{X_1, X_2\}$, the graphical view of the country's ES level is presented in Fig. 2 [9].

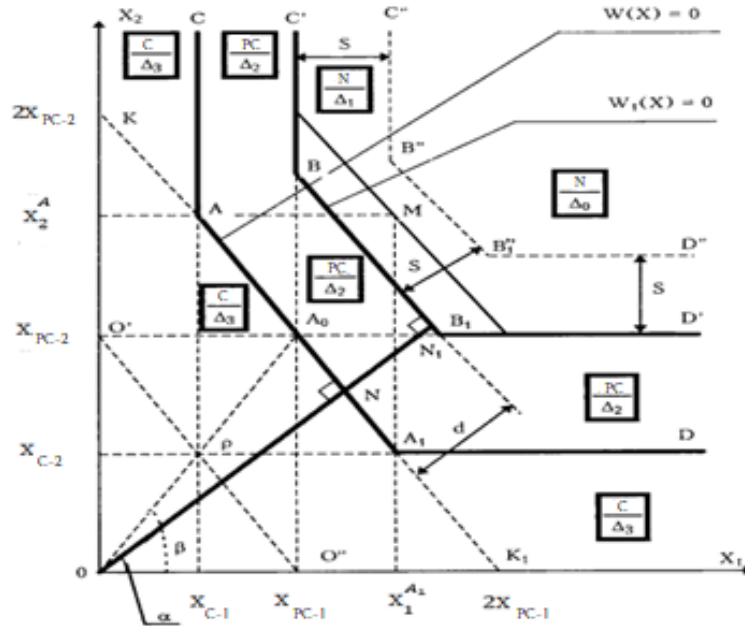


Fig. 2. Graphic Image of the Method of Intersecting Planes for ES Level Assessment

where Δ_0 , Δ_1 , Δ_2 and Δ_3 are respectively the levels of N in ES, but there are significant risks of situational change in normal (N), pre-crisis (PC) and crisis (C) situations.

If we separate the N, PC and C zones of the ES level from each other by planes, then the situational zone for the indicator will be described at a distance from the S point, and up to the next dividing plane will describe the current state of the indicator.

Guided by the principle of ensuring a stable level of country's ES, the fluctuation in the level of indicators should be restricted to surface limited with lines C'BB₁D' and C''B''B₁''D'' [10].

In case of crisis situation, the following restrictions are applied:

$$X_i \leq X_{PC,i}, i=1, \dots, m, W(X_1, X_2, \dots, X_m) \leq 0. \quad (7)$$

In case of pre-crisis situation the following restrictions are applied:

$$X_{C,i} \leq X_i \leq X_{PC,i}, i=1, \dots, m, W(X_1, X_2, \dots, X_m) > 0, W_1(X_1, X_2, \dots, X_m) \leq 0. \quad (8)$$

In case of normal situation, the following restrictions are applied:

$$X_i > X_{PC,i}, i=1, \dots, m, W_1(X_1, X_2, \dots, X_m) > 0. \quad (9)$$

To assess the country's ES level, a system of intersecting planes for indicators characterizing the situation must be created and mathematical addition or division for each of the two indicators must be performed.

$$X_1 X_{PC,2} + X_2 X_{PC,1} = X_{PC,1} X_{PC,2}. \quad (10)$$

Since the line KAA₀A₁K₁ is parallel to the line O'O" and passes through the point A₀(X_{PC,1}, X_{PC,2}), thus O''K=X_{PC,1}, and O''K=X_{PC,2}. To determine the coordinates of the points A and A₁, it is necessary to consider the fact that point A₁ lies on the line KAA₀A₁K₁, so the following expressions are correct:

$$(2X_{PC,1})^{-1} X_1^{A_1} + (2X_{PC,2})^{-1} X_{C,2} = 1. \quad (11)$$

The coordinates of point A can be determined in the same way.

Now considering the following 3 points on the same line A(X_{C,1}, X_{C,2}^A), A₀(X_{PC,1}, X_{PC,2}), A₁(X₁^{A₁}, X_{C,2}), the following connection can be made for them:

$$\begin{bmatrix} X_{C,1} & X_2^A \\ X_{PC,1} & X_{PC,2} \\ X_1^{A_1} & X_{C,2} \end{bmatrix} = 1. \quad (12)$$

As it is known in multidimensional space the planes $W(X) = 0$ and $W_1(X) = 0$ are parallel if $(A'/A'') = (B'/B'') = \dots = (C'/C'')$. If the parameters of the plane $W_1(X) = 0$ are the same as the plane $W(X)$, they will differ from each other only by a free term of an equation, which characterizes the distance of the plane from the coordinate axis, and the distance between the two planes can be determined as follows [11]:

$$d = |H'' - H'| / ((A')^2 + (B')^2 + \dots + (C')^2)^{1/2}. \quad (13)$$

In order to fully analyze the indicators characterizing the ES level, it is also necessary to introduce crisis values ($X_{C,i}$, $i = 1 \dots m$) and pre-crisis limit values ($X_{PC,i}$, $i = 1 \dots m$) in the presented methodology.

The discriminant analysis method is based on the theory of image recognition, in the ES level study, if the calculation value of describing indicators is known but their limit values are unknown, then the country's ES level can be classified based on the statistics.

If the function of the classified indicators is denoted $E(X)$ and if $E(X_1, X_2 \dots X_m) = 0$ then there is a plane dividing crisis and pre-crisis situations, and if $E_1(X_1, X_2 \dots X_m) = 0$ then there is a plane dividing pre-crisis and normal situations and the following can be given:

$$K \in \begin{cases} A_C, \text{ if } E(X) \geq 0, X_i \geq X_{C,i} \\ A_{PC}, \text{ if } E_1(X) \geq 0, E(X) \geq 0, X_{C,i} > X_i \geq X_{PC,i} \\ A_N, \text{ if } E_1(X) < 0, X_i < X_{PC,i} \end{cases} \quad (14)$$

In order to determine the ES level, it is necessary to use a probabilistic method, which corresponds to the situation when the dividing planes coincide.

If for the situation $A(X_h)$ the X_h forms $h = C, PC, N$ are known, then the recognition of the unknown $a(X_0)$ situation with the parameters X_0 is performed as follows:

$$X_0 \in X_h \Rightarrow a(X_0) \in A(X_h), \quad h = C, PC, N. \quad (15)$$

Two types of errors are possible during the study - $(P_1(K))$ is the absence of response and $(P_2(K))$ is false response.

To reduce these errors, formulate the reduction function $F(K)$ under the given q_h ($h=1,2$) conditions, which will be called the Bayesian method, which is the following:

$$F(K) = c_1 q_1 P_1(K) + c_2 q_2 P_2(K), \quad (16)$$

where q_h ($h=1,2$) is the probability of two situations occurring together, c_1 and c_2 is the value "paid" as a result of the error.

The rule K of determining the function $F(K)$ has the following form:

$$K_1 \begin{cases} X \in R^m, \frac{P_1(X)}{P_2(X)} \geq \frac{c_2 q_2}{c_1 q_1}, \\ X \in R^m, \frac{P_1(X)}{P_2(X)} < \frac{c_2 q_2}{c_1 q_1}, \end{cases} \quad (17)$$

The G_j functionals will be determined as follows:

$$G_j = \lg(c_j q_j) - 1/2(X - M_j)^T S_j^{-1} (X - M_j) - 1/2 \lg |S_j|. \quad (18)$$

Under normal distribution conditions, situation X can be considered as a part of the set of situations $A(X_1)$ if:

$$(\lg(c_1 q_1) - 1/2(X - M_1)^T S_1^{-1} (X - M_1) - 1/2 \lg |S_1| - \lg(c_2 q_2) - 1/2(X - M_2)^T S_2^{-1} (X - M_2) - 1/2 \lg |S_2|) \geq 0 \quad (19)$$

where M_h and S_h are the mathematical expectation of the parameters of order h and the covariance matrix, respectively.

M and S assessments are determined as follows:

$$M = \frac{1}{N} \sum_{j=1}^N X_j, \quad (20)$$

$$S = \frac{1}{N-1} \sum_{j=1}^N (X_j - M_j)(X_j - M_j)^T. \quad (21)$$

Taking into account the equation (9) we can write the linear discriminant function of G_j that has the following form:

$$E(X) = X^T S^{-1} (M_1 - M_2) - 1/2(M_1 + M_2)^T S^{-1} (M_1 - M_2) - \lg(c_2 q_2 / c_1 q_1) = 0, \quad (22)$$

where $E(X)$ is the linear discriminant function, and $B = S^{-1} (M_1 - M_2)$ is the discriminant vector, which is the normal of the H hyper plane.

The linear discriminant function is determined as follows:

$$E(X) = B^T X - G = 0. \quad (23)$$

If the actual distribution does not have a normal form, a linear discriminant function can be defined as the Fisher function minimizing the distance between two wholes.

$$F = \frac{(M_1 - M_2)}{\sigma^2}, \quad (24)$$

where $M_i = B^T M_j$ is the projection of the j whole on the vector B , $\sigma^2 = B^T S B$ is the dispersion of the projected wholes.

As a result, differentiating the function F according to B , we will get the same vector.

Using the discriminant method to characterize the ES situation, it can be presented as an equation of the plane passing through the intersections describing the situation and the hyperplane of the existing situation perpendicular to it.

$$(M_1 - M_2)^T X - 1/2(|M_2|^2 - |M_1|^2) = 0. \quad (25)$$

Since the indicators characterizing ES can have different measurement units that are in some cases incompatible, we will present the indicators in a standardized form [12].

$$X_i^0 = \frac{X_i - M(X_i)}{\sigma(X_i)}, \quad (26)$$

where $M(X_i)$ and $\sigma(X_i)$ are the mathematical expectation of the indicators and average squared deviations, respectively.

Thus, it can be said that the characteristic of the ES situation are the importance coefficients of the indicators that form this situation, as a result of which the ES level and its characteristic situation will be determined as follows:

$$M_{ESI} = N^{-1} \sum_{i=1}^N X_i, \forall X_i \in A_h. \quad (27)$$

The method of fuzzy sets is based on the principle of continuity of situations characterizing the ES level, and an exponential function is used to solve the problem.

$$f(x) = \exp[b(x-c)^2], \quad (28)$$

where b and c are the parameters that determine the image of the function.

The recognition of the given situation is carried out by the continuation of the situations characterizing the levels of indicators characterizing ES based on the following equation:

$$\gamma_s = \max_k \{ \min_i \{ \sup_{x \in X} (\min \{ \mu_i(x), V_{sik}(x) \}) \} \}, \quad (29)$$

where γ_s is the continuity of the observed situation s , X is the range of values of the indicators i , $\mu_i(x)$ is the function of the continuity of observed situation i , V_{sik} is a function of the continuity of k assumption presented by the professional group in relation to the observed situation s of i indicator.

Results and discussions

Examining the most common methods of ES level assessment, it can be noticed that they are mostly based on a system of indicator determination, which aims to develop a reliable schedule-program for the provision of the country's energy resources and for increasing their management efficiency and consumption continuity.

The principle of individual analysis of indicators is mostly applied in methodologies for estimating the observed ES level, at the same time the conclusion about the country's ES level is made on the basis of absolute or relative differences of the values obtained in the calculation and base periods.

Conclusion

Four methodologies for assessing the level of ES were considered, which are based on the principle of indicator analysis. For the purpose of assessing the level of ES, as a result of the research, in order to assess the level of energy security of the Republic of Armenia with the mentioned models, it was proposed to improve the methodologies of assessing the level of ES in the following directions:

1. In the case of the scaling method, the methodology used to assess the level of ES is based on the weight of the capacity, it was suggested to use in addition to the principles of scaling the relationship between the indicators characterizing the level of ES, which is presented in the form of a system of equations, the sum of the free members of which is limited with the $\sum_{i=1}^n K_i = 1$ expression. The values of the free members are formed based on the results of the carried out capacity calculations.
2. In the case of applying the method of intersecting planes, the methodology used to assess the level of ES is carried out based on the situational analysis of the indicators characterizing the level of ES. At the same

time, there is significant complexity in the application of the method, which becomes more obvious when the problem under consideration is not meet the requirements of the two-dimensional plane, it is recommended to use this method after determining the weight of the indicators characterizing the level of ES, using higher efficiency as a primary indicator which are more significantly correlated with other indicators, at the same time creating the opportunity to solve the given problem more quickly.

3. Discriminatory analysis and methods of indeterminate multitude are based on an artificial intelligence software system endowed with the feature of individual decision making, however, the main disadvantage of these methods is that the decision is made on the basis of the continuity of the ES level situation or the process of their recognition based on statistical data. It is proposed to assess the level of EA as a result of the joint application of the methods based on statistical data and their continuity, as a result of which it will be possible to clearly distinguish the situation zone of the ES level and to make an operative decision.

References

- [1]. V.V. Bushuev, N.I. Voropay, A.M. Mastepanov, Yu.K. Shafranik et al, Energeticheskaya bezopasnost' Rossii. Novosibirsk: Nauka. Siberian Publishing Company RAS, 1998 (in Russian).
- [2]. A.M. Filipchenko, On the issue of the essence, content and mechanism of ensuring the energy security of the state – Moscow. Finance and Credit, 1, 2005, 55-68.
- [3]. A.T. Myzina, A.A. Kuklina, Sectoral and regional problems of the formation of energy security. Institute of Economics of the Ural Branch of the Russian Academy of Sciences, Ural, 2008.
- [4]. L.L. Bogatyrev, A.I. Tatarkina, A.M. Mostepanov, Methodology for diagnosing the economic and energy security of the state. Institute of Economics of the Ural Branch of the Russian Academy of Sciences, Yekaterinburg, 2003.
- [5]. F. Umbach, The global energy securities and implication for the EU. Energy Policies, 39 (4), 2010, 1229-1241.
- [6]. V.A. Saveliev, Methodology for assessing the energy security of regions on the example of the Ivanovo region, in: Improving the efficiency of power systems. Tr. ISEU, Energoatomizdat, Moscow, 5, 2002, p.100.
- [7]. K.S. Zykov, Energy security as a component of Russia's economic development, Proceedings of the International Research and Production Complex on Economic and Energy Security of Russian Regions, Part I, Perm, 2003.
- [8]. A.I. Tatarkin, The influence of the energetic factor on the economic security of the regions of the Russian Federation, Management Academy, Yekaterinburg, 1998.
- [9]. G. Bahgat, Energy Security: An Interdisciplinary Approach, first ed. , Indiana University of Pennsylvania, Wiley, 2011.
- [10]. L.D. Gitelman, B.E. Ratnikov, Effektivnaya energokompaniya: ekonomika, management, reformirovanie. Olimp-Biznes, Moscow, 2002.
- [11]. E.V. Bykova, Methods for Calculation and Analysis of Energy Security Indices. Chisinau: CEP USM, Institute of Power Engineering, 2005.
- [12]. G.B. Maria, Managing energy security an all hazards approach to critical infrastructure, first ed. , Routledge, New York, 2019.

Khachik Arthur Shahbazyan (RA, Yerevan) - National Polytechnic University of Armenia, lecturer at the Chair of the Economics and Management in the Field of Energy, Kh.shahbazyan95@gmail.com

Submitted: 14.04.2021

Revised: 25.05.2021

Accepted: 03.06.2021

UDC 628.334.51, 628.543
DOI: 10.54338/27382656-2021.1-8

Varuzhan Levon Shamyán

National University of Architecture and Construction of Armenia, Yerevan, RA

USE OF VARIOUS THIN-LAYER SETTLING SCHEMES FOR INDUSTRIAL WASTEWATER TREATMENT

In this paper, the theoretical preconditions in favor of the use of thin-layer settling tanks for industrial wastewater treatment are substantiated by the corresponding laboratory studies. The data from the results of studies of wastewater treatment of the textile, knitwear and silk industries conducted on laboratory thin-layer settling tanks according to the basic schemes of wastewater supply and precipitating sediment are given. As stated by these data, according to the generally accepted criteria for the effectiveness of suspended solids retention for wastewater of the above-mentioned industries, it is more preferable to use thin-layer sedimentation in a cross-sectional scheme.

Keywords: *suspended matter, laminar flow, inter-shelf distance, flow velocity.*

Introduction

The relative simplicity of the settling facilities and the settling process itself, low energy intensity and availability precondition their widespread use at various stages of wastewater treatment and sediment processing. In our case, the sedimentation is used for preliminary industrial wastewater treatment and is carried out in thin-layer settling tanks. Despite the fact that a lot of researchers have studied the issues of thin-layer settling [1...9, etc.], to this day there are no definite recommendations for identifying the optimal scheme for industrial wastewater treatment in a particular sector of the national economy. Therefore, the studies to determine the optimal structural parameters of thin-layer settling tanks and the optimal technological parameters of the settling process are relevant both from the point of view of choosing the appropriate type of structure and its operation scheme, as well as from the possibility of preliminary classification of characteristics of suspended matter (shape and size of particles, density, rate of their sedimentation and the ability to agglomerate, etc.) of wastewater of the industries under study.

Main Part

In order to improve the operation of the settling tanks by constructive methods, Hazen A. developed a theory [1], according to which the division of the general settling zone into a number of elementary zones with a lower depth simultaneously increases the sedimentation area (up to 0.80) according to the data of the works [2...8], and also allows significant increase in the hydraulic load per unit area, thereby providing more effective clarification, the productivity of which increases proportionally to the sedimentation area on average 2 ... 4 times [9]. Thin-layer settling tanks, like the regular ones, have water distribution, settling and catchment zones, as well as a sedimentary zone. The settling zone is divided by parallel shelves (or pipes) and settling is carried out in the space between the shelves with a height of 2 ... 15 cm. As a result of reducing the path for the sedimentation of suspended matter, the settling process in thin-layer settling tanks occurs very quickly in 15 ... 30 minutes, the sizes of thin-layer settling tanks are reduced 4 ... 6 times, which makes it possible to construct them even in enclosed spaces [9, 10]. The temperature within the layer is more uniform, the turbulence of flow is minimized, and the hydraulic conditions of settling and separation of sediments are improved.

The hydrodynamic stability of suspended matter is also increased in thin layer settling tanks, and the influence of density and convection flows on the process of settling the suspended matter is minimized. In addition to creeping forces, additional forces of suspension drift on thin-layer elements appear. As a result of dividing the flow by separate elements, the amplitude and frequency of the flow velocity pulsation of the

treated wastewater also attenuate, the wetted perimeter significantly increases, and conditions that will contribute to the maximum laminar flow of liquid in thin-layer elements are created*.

It is known that non-pressure flows can be characterized by the ratio of inertial forces to gravity forces, which is the Froude number (Fr):

$$Fr = V^2 / g \cdot h \geq 10^{-5}, \quad (1)$$

where V is the average flow velocity, m/s ; g is the acceleration of gravity, m/s^2 ; h is the average flow depth (in our case, the inter-shelf height), m .

Flow stabilization is possible if the energy of water particles movement prevails over the gravity forces. Flow stability is always ensured at $Fr \geq 10^{-5}$. The values of Froude number give us reason to believe that the flow structure in the settling tanks cannot be formally described only by Reynolds numbers (Re):

$$Re = V \cdot R / \nu \leq 500, \quad (2)$$

where R is the hydraulic radius, m ; and ν is the kinematic coefficient of viscosity, m^2/s .

Equations (1) and (2) are presented for the laminar fluid movements in thin-layer elements, at which the optimal operation mode of thin-layer settling tanks is achieved. Despite the more rigid structure of the tubular elements, which ensures dimensional consistency over the entire length and can operate at higher speeds, they are quicker to fill up with sediments, more difficult to clean and require higher material consumption. Therefore, in the studies carried out, preference was given to shelves, which are mounted from flat or wavy plates convenient in operation.

For shelf settling tanks $Re \approx h$ and dependence (2) takes the form

$$Re = V \cdot h / \nu \leq 500. \quad (3)$$

The maximum available velocity of fluid movement in thin-layer elements, based on condition (2) and at $Re \leq 500$ should be:

$$V_{max} \leq 500 \cdot \nu / h. \quad (4)$$

The study was carried out on two laboratory units of rectangular and circular cross-sections designed and mounted by the author of the paper, for application of flat plates made of galvanized sheet and plastic, providing easy sliding and removal of sediment from the surface.

The laboratory unit of thin-layer rectangular cross-section is a plexiglass prism open from the top with dimensions of $100 \times 200 \times 500 \text{ mm}$. From above this prism is immersed in rectangular prismatic frame, in which sets of shelving elements made of a galvanized sheet (0.8 mm thick) and from plastics (1.0 and 1.2 mm thick) were applied. Galvanized sheets assembled in a rectangular prismatic frame are shown in Fig. 1, and sets of plastic plates are shown beside. Plate sets made of these materials are designed for studies of settling of suspended matter from wastewater at an angle of $55 \dots 65^\circ$ relative to the bottom of the laboratory settling tank. There is also a rectangular prismatic frame made of plastic with flat elements of galvanized sheet assembled at an angle of $45 \dots 55^\circ$ relative to the bottom of the laboratory settling tank.

Installation of a thin-layer rectangular settling tank is shown in Fig. 2.

The feed rate is controlled by a valve located on the pipe just in front of the inlet to the thin-layer settling tank. A branch pipe with a valve for periodic sediment discharge and emptying of the thin-layered settling tank into a bucket is located on the right side next to the sewage pipe. Occasionally, the experiments were performed

* <https://stowater.com/katalog-oborudovaniya/otstojnik-tonkoslojnyij.html>
https://prom-water.ru/catalog/ochistka_stochnyh_vod/otstojniki/

with a perforated panel (shown in the image below on the left side before the measuring cylinder), which was placed vertically near the frame of the shelf elements in order to maximize the laminarization of the wastewater supply. The clarified wastewater is drawn off from the surface through a 15 mm hose. Three other hoses having clamps at the end with a diameter of respectively 12; 8 and 5 mm, immersed in liquid, are designed for taking samples from different heights of the laboratory settling tank.

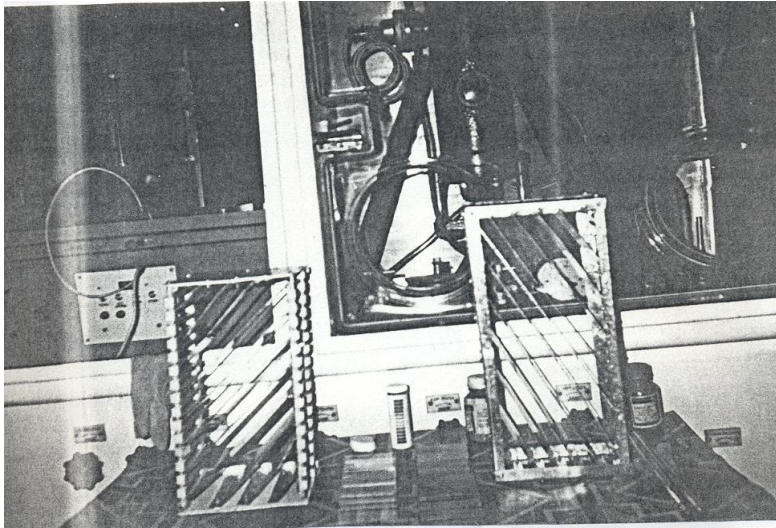


Fig. 1. *Prismatic frames with thin-layer elements*

the stream under study will flow from the top of a container with a volume of 42.5 liters with dimensions of $500 \times 340 \times 250$ mm. The frame of the circular section unit is a steel cylinder with an inner diameter of 140 mm and a height of 500 mm. At a height of 360 mm on the left side, there is a branch pipe with a clamp at the end of the hose, through which it is also possible to supply the treated wastewater thus conducting part of the experiments of thin-layer settling in a cross-scheme. But in general, this unit is designed to carry out experiments of thin-layer settling tanks in a countercurrent scheme. To do this, the treated wastewater is supplied by a hose (10 mm) from a cylindrical container located on the top, with a volume of 42.5 liters (diameter 300 mm and height 600 mm) through the central bottom pipe branch to the laboratory settling tank.



Fig. 2. *Laboratory unit of a thin-layer settling tank (rectangular section)*

In the cross - flow scheme study, the wastewater is supplied through a 12 mm lateral central connecting pipe with a plug, which is connected to a transparent hose of the same diameter (the longest in the image). Wastewater is also supplied through a 50 mm metal pipe displayed on the foreground, with a 10 mm connecting pipe mounted to it. At the end of the connecting pipe, a connected piece of a submerged hose of the same diameter directs the wastewater stream to the left lateral side of the unit. In both cases,

The clarified wastewater is discharged from the top through a 10 mm hose on the right side, from where periodically a sample is taken to determine the effectiveness of the treatment according to the main indicators. The located upper central branch pipe with a hose and a clamp can also be used for supplying treated wastewater. In this case, if the lower central pipe is disconnected, the laboratory unit will work according to a direct flow scheme of wastewater and sediment removal. The recurrent sediment is removed through the brown hose with a clamp, the beginning of which is located 30 mm above the level of the unit bottom. The dynamics of the sediment accumulation and the whole process of wastewater clarification can be monitored through a cutout transparent window with a diameter of 55 mm.

Fig. 3 shows two sets of oval shelf elements made of galvanized sheets and plastic. Each set of flat elements has

been mounted at angles from 45° to 65° (as in the case of the rectangular prism) with a gap in order to avoid obstacles to the settling process itself. At the same time, this distance contributed in part to the laminarization of the flow in the thin-layer elements as a distribution zone. Thin-layer oval elements were installed into the unit, starting from a level just above the transparent window to a level of 5 cm below the clarified wastewater at a distance of $2 \dots 10\text{ cm}$ between themselves.

From above, the height of the entire thin-layer settling tank can be extended by a flanged connection, thereby providing more accurate technical data on the sedimentation of suspended matter. Fig. 3b shows the general appearance of a thin-layer settling tank extended by additional 550 mm .

The basic schemes of reciprocal movement of wastewater and released sediment are the following: cross-sectional scheme - when the selected sediment moves perpendicularly to the movement of the fluid flow; countercurrent scheme - the discharged sediment is removed in the direction opposite to the movement of the fluid flow; direct-flow scheme - direction of the sediment movement coincides with the direction of water flow. In fact, two laboratory units could be used for cross-sectional studies (prism unit) and for direct or countercurrent scheme (cylindrical unit) of thin-layer settling.

All experiments were carried out at optimal values of the wastewater flow velocity of ($V = 5 \dots 10\text{ mm/s}$) and the inclination angle of the plate elements ($\alpha = 55^\circ$) obtained by the author in advance for the observable wastewater. The inter-shelf distance was taken $h = 2 \dots 10\text{ cm}$, at which, according to conditions of (1) and (3) (or (4)), a laminar flow in thin-layer elements was theoretically ensured.



a



b

Fig. 3. Laboratory unit for thin-layer settling

a - circular cross-section; b - elongated version of circular cross-section

In general, thin-layer settling tanks are effective in extracting finely dispersed impurities from wastewater, which is typical for wastewater from silk, textile and knitwear industries. The data from the cross sectional scheme studies are shown in Table. 1, while the data from direct and countercurrent scheme studies are shown in Table. 2, where the maximum treatment efficiency values are presented.

Table 1. Indicators of wastewater treatment after thin – layer settling by direct-flow scheme and countercurrent scheme

Main characteristics	Industrial wastewater					
	textile			knitwear		
	before treatment	after thin-layer settling/ effect, %		before treatment	after thin-layer settling/ effect, %	
		direct flow scheme	countercurrent scheme		direct flow scheme	countercurrent scheme
suspended matter, mg/l	120...180	$\frac{54...81}{55}$	$\frac{48...72}{60}$	32...320	$\frac{14...140}{56}$	$\frac{13...130}{62}$
COD, mg/l	450...900	$\frac{337...674}{25}$	$\frac{315...630}{30}$	880...2600	$\frac{642...1898}{27}$	$\frac{581...1716}{34}$
BOD, mgO ₂ /l	160...340	$\frac{125...265}{22}$	$\frac{120...255}{25}$	200...500	$\frac{152...380}{24}$	$\frac{146...365}{27}$
pH	8.5...10.0	9.1	9.2	6.5...9.0	7.8	7.9

According to the Table. 1, it can be confirmed that the effectiveness of suspended solids retention is from 5 to 7% higher in the countercurrent scheme compared to the direct-flow sedimentation scheme. This is due to the fact that favorable conditions are created for suspended solids settling in shorter trajectories when the wastewater moves up in inclined plates from the bottom.

Table 2. Indicators of industrial wastewater treatment after thin-layer settling in a cross-section scheme

Main characteristics	Industrial wastewater					
	textile		knitwear		silk	
	before treatment	after thin-layer settling / effect, %	before treatment	after thin-layer settling / effect, %	before treatment	after thin-layer settling / effect, %
Suspended matter, mg/l	150	$\frac{67}{58}$	290	$\frac{104}{64}$	260	$\frac{96}{63}$
COD, mg/l	610	$\frac{439}{28}$	1100	$\frac{726}{34}$	850	$\frac{578}{32}$
BOD, mgO ₂ /l	220	$\frac{165}{25}$	340	$\frac{148}{27}$	365	$\frac{266}{27}$
pH	8.6...9.8	9.2	6.8...9.1	7.9	7.6...9.0	8.2

Comparison of the data in Table. 1 and Table 2 shows that wastewater treatment in the aforementioned industries by thin-layer sedimentation is preferable to be performed using a cross-sectional scheme, in which the effectiveness of the retention of suspended solids is on average increased by additional 1 ... 2%.

Outcomes

From the above-mentioned it follows that:

1. The treatment of wastewater from textile, knitwear and silk industries by thin-layer settling is almost the same, and high efficiency is provided by cross-section flow and countercurrent flow schemes,
2. The tendency of higher effectiveness of retention of suspended substances at their proportionally high initial values was confirmed for all three thin-layer settling schemes.

Conclusion

The cross-section flow scheme primarily implies the realization of the process in horizontal, thin-layer settling tanks with a detailed calculation of the distribution zone length of the structure.

It should be noted that the effectiveness of thin-layer sedimentation depends not only on the adopted scheme but also on other structural parameters [11, 12]. In particular, it is also important that the flow is distributed evenly among all thin layer elements. For this purpose appropriate proportional distribution should be provided in the laboratory units, similar to Fig. 4 and additional studies should be conducted for wastewater of the industries under study.

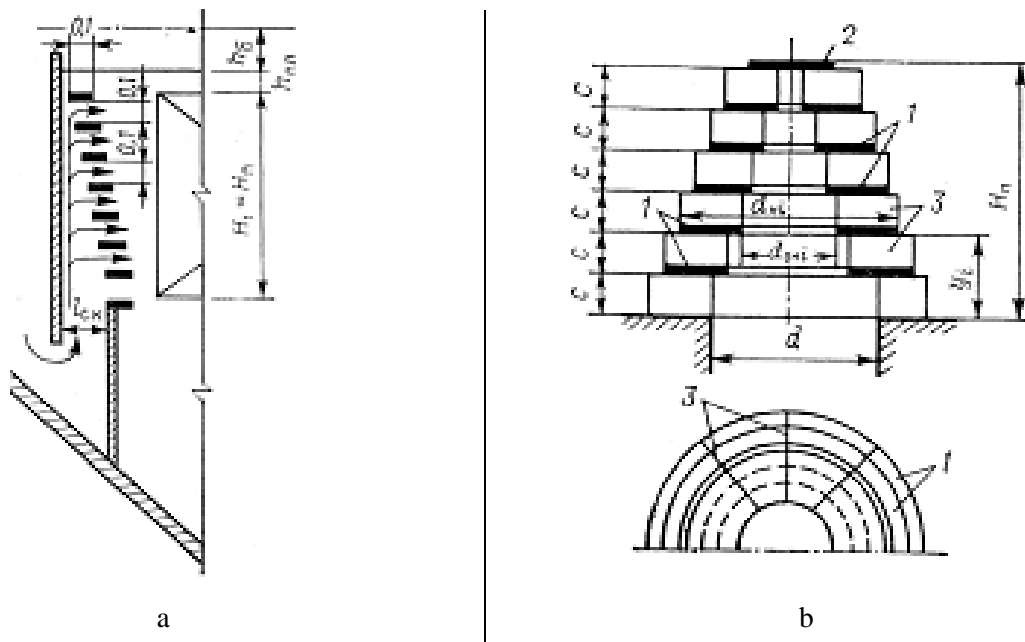


Fig. 4. Proportional distribution devices

a - in a cross-section scheme; b - in a countercurrent scheme based on the principle of flow differentiation; 1 - disc annular; 2 - the same, solid; 3 - radial directing baffles

Among the technological parameters, we may note the need to use various reagents for the discoloration and retention of surfactants of the wastewaters under study, as well as the possibility of some increase in the flow velocity [13, 14] in order to identify the optimal combination of values between duration and efficiency of settling for suspended substances.

References

- [1]. A.Hazen, On Sedimentation. Transactions of the American Society of Civil Engineers, 53 (2), 1904, 45-71.
- [2]. V.A. Klyachko, B.E. Lieberman. Thin-layer multitier lamellar sedimentation tank. Water supply and sanitary engineering, 11, 1976, 25-26.
- [3]. Yu.M. Simonov, V.G. Ivanov, M.S. Pavlov, Testing of thin-layer sedimentation tanks on low-color water of medium turbidity. Water supply and sanitary engineering, 1, 1979, 24-26.
- [4]. V.I. Kalitsun, Yu.M. Laskov, Laboratory workshop on sewerage. Stroyizdat, Moscow, 1978.
- [5]. V.G. Ivanov, V.P. Semenov, Yu.M. Simonov, The use of thin-layer sedimentation tanks in the pulp and paper industry. Timber industry, Moscow, 1989.
- [6]. V.L. Shamyán, Technological and constructive proposals on sand trap and removal from industrial and domestic waste water. Advanced Materials Research, 1020, 626-630.
- [7]. V.L. Shamyán, features of the calculation of thin-layer settling tanks. Bulletin of Ysuac, 3, 2008, 270-273.
- [8]. T.I. Baryshnikova, V.A. Radtsig, Thin-layer sedimentation tanks. Chelyabinsk Polytechnic Institute, Chelyabinsk, 1983.
- [9]. M.V. Demura, Design of thin-layer sedimentation tanks. Budivelnik, Kiev, 1981.
- [10]. G.V. Vasiliev, Yu.M. Laskov, E.G. Vasileva, Water management and waste water treatment of Enterprises of the textile industry, Light industry, Moscow, 1976.
- [11]. V.L. Shamyán, Influence of the angle of inclination of thin-layer elements on the efficiency of retention of suspended solids. Energy saving and water treatment, 2, 2000, 92-94.

- [12]. V.L. Shamyán, Constructive proposals for thin-layer sedimentation. Scientific works of Ysuac, 2 (28), 2006, 125-127.
- [13]. V.L. Shamyán, N.A. Trunova, Influence of the rate of supply of waste water into a thin-layer clarifier on the efficiency of sedimentation of suspended solids. Housing construction, 11, 1998, 22-23.
- [14]. V.L. Shamyán, Determination of the optimal flow rate of waste water during reagent thin-layer sedimentation, Construction – formation of vital activity of the living environment. Materials of the 3rd scientific-practical conference, Moscow, 2000, 80-82.

Varuzhan Levon Shamyán, doctor of philosophy (PhD) in engineering, associate professor (RA, Yerevan) - National University of Architecture and Construction of Armenia, associate professor at the Chair of Hydroconstruction, Water Systems and Hydroelectric Power Plants, armsham_05@yahoo.com

Submitted: 18.03.2021

Revised: 24.03.2021

Accepted: 31.03.2021

REQUIREMENTS FOR FORMULATING SCIENTIFIC ARTICLES AND THE SUPPORTING DOCUMENTS

1. Papers can be submitted in English (3-10 pages)

Mandatory electronic documents should be submitted with site.

<https://jaer.nuaca.am/?journal=jaer&page=about&op=submissions>

The paper (paper in *.doc, *.docx format, illustrations in *.jpg, *.jpeg, *.png format).

Font: Times New Roman, **style:** normal

Parameters of page

- A4 format (210 x 296 mm)
- Margins: 20mm from left, right, top and bottom
- Indentions – 0.5 mm
- Spacing between lines – Multiple – 1.2

2. Article Formulation Requirements:

The article should have the following structure

The Title of the Article

It should briefly (no more than 10 words) and accurately reflect the subject of scientific research. The title should reflect the uniqueness of the author's scientific work.

Abstract

Must contain (up to 150 words) the following brief information about the submitted article:

1. description of the subject (object) of the study, the purpose and objectives, actuality, novelty and practical significance of the scientific research,
2. method (s) and methodology (if possible),
3. scientific results obtained (theoretical and experimental results, factual data, discovered relationships and patterns),
4. recommendations, assessments and proposals.

Keywords

Keywords are the way to search for a scientific article, as in all *international bibliographic databases* articles can be searched by keywords. In this regard, they should reflect the basic terminology of scientific research. It is necessary to include 3-8 keywords.

Introduction

The objective of Introduction - overview of the current state of the observed issues of the article, significance of scientific problems and its actuality.

Introduction should include a review of modern Armenian and foreign scientific achievements in the subject area, research and the results on which the work is based (Literature review). The literature review should emphasize the actuality and novelty of the issues considered in the study, on the basis of which the goals and objectives of the given work are set and described. The reference numbers to the source cited in the text are placed in square brackets strictly in sequence like [1], [2], ...

Introduction should contain information that will allow the reader to understand and evaluate the novelty and actuality of the research results presented in the article.

Materials and Methods

This section should clearly describe the methodology of the study. Formulas and mathematical expressions

should be written in Microsoft Equation or MathType, Italic, 11 pt. The formulas are presented in a separate line, in the middle, and the main formulas are numbered on the right, in the form (1), (2), ...

Results and Discussion

In this part of the article, a systematic authorial analytical and statistical material should be presented. The results of the study must be described so that the reader can trace its stages and assess the validity of the conclusions made by the author. The main purpose of this section is summarizing and clarifying data to prove the working hypothesis (hypotheses) through analysis. The results, if necessary, are confirmed by tables, graphs, figures, which represent the source material or evidence. It is desirable to compare the results presented in the article with previous works in this area by both the author and other researchers. Such a comparison will additionally reveal the novelty of the work done, giving it objectivity.

Conclusion

Conclusion contains a brief description of the *Materials and Methods* section, as well as a brief statement of the research results. Here in compressed form, the main thoughts of the *Results and Discussion* section are repeated. In this section, it is necessary to compare the results obtained with the goal indicated at the beginning of the work. In Conclusion, the results of comprehension of the topic are summarized, conclusions, generalizations are made, and recommendations arising from the work are given, their practical significance is emphasized. In the final part of the article, it is desirable to include the prospects for the development of the research in this area.

Acknowledgments (if necessary)

This section, we refer to those persons who have assisted in the implementation of the study and those organizations that provide financial assistance.

References

The list of references should include from 10 to 30 sources (self-citations should be avoided), not taking into account references to regulations and internet resources. It is not recommended to refer to Internet resources that do not contain scientific information, textbooks, training and methodological manuals. It is known that the level of publication is determined by the completeness and representativeness of the sources; therefore, it is recommended to refer first of all to original sources from scientific journals included in the global citation indexes (Web of Science / Scopus). The sources should be relevant (mandatory use of original sources no older than 10 years).

The sources included in the References should be compiled according to «*Numbered style*» standard of Elsevier scientific publishing company.

Examples of presenting sources included in the References:

Please, note the DOI-s of articles if possible and provide the transliteration of the references, that are not in latin script.

Journal article

- [1]. A.Hazen, On Sedimentation. Transactions of the American Society of Civil Engineers, 53 (2), 1904, 45-71.
- [2]. K.S. Gyunashyan, R.R. Sinanyan, Ye.H. Hayrapetyan, Constant "K" of the CD-1200 light range finder and the results of production tests. Geodesy and aerial photography, 4, 1996, 136-143.
- [3]. J. van der Geer, J.A.J. Hanraads, R.A. Lupton, The art of writing a scientific article. J. Sci. Commun., 163 (3), 2000, 51-59.
- [4]. M.M. Badalyan, Cementless concretes based on raw materials from Buryatia. Bulletin of Builders of Armenia (special issue), 8, 1999, 8-9.

- [5]. T.V. Grunskoy, V.P. Perkhutkin, A.G. Berdnik, Analytical review of working conditions of underground personnel in the oil mines of the Yaregskoe Field. Perm Journal of Petroleum and Mining Engineering, 16 (4), 2017, 378-390.
- [6]. E.A. Hayrapetyan, S.K. Petrosyan, V.G. Harutyunyan, A.A. Khachatryan, Vybora modulyatora sveta etalonnogo svetodal'nomena. Bulletin of National University of Architecture and Construction of Armenia, 1, 2020, 50-57 (in Russian).
- [7]. V.D. Eryomin, Opredelenie chastot i form sobstvennykh kolebaniy obolochek neklassicheskoy formy. Scientific papers of National University of Architecture and Construction of Armenia, 1, 2015, 94-100 (in Russian).

Book

- [1]. Z.A. Atsagortsyan, Natural stone materials of Armenia. Stroyizdat, Moscow, 1967.
- [2]. E.E.R. Mustel, V.N. Parygin, Methods of modulation and scanning of light. Nedra, Moscow, 1970.
- [3]. W. Strunk Jr., E.B. White, The Elements of Style, third ed. Macmillan, New York, 1979.
- [4]. A.N. Zavaritskiy, Igneous rock. USSR Academy of Sciences, Moscow, 1960.
- [5]. A.L. Goldenveiser, Teoriya uprugikh tonkikh obolochek. Nauka, Moscow, 1976 (in Russian).
- [6]. L.V. Kantorovich, V.I. Krylov, Priblizhennyye metody vysshego analiza. Fizmatgiz, Moscow, 1962 (in Russian).

Book chapter

- [1]. G.R. Mettam, L.B. Adams, How to prepare an electronic version of your article, in: B.S. Jones, R.Z. Smith (eds.), Introduction to the Electronic Age. E-Publishing Inc., New York, 1999, 281-304.
- [2]. G.A. Tiratsyan, Transcaucasia, in: B.A. Rybakov (ed.), The most ancient states of the Caucasus and Central Asia, Nauka, Moscow, 1985, 482-568.

Conference Paper

- [1]. A.G. Beglaryan, K. S. Gyunashyan, Ye.H. Hayrapetyan, High precision light range-finder DVCD-1200 for linear comparator. Proceedings of 3rd international conference on contemporary problems of architecture and construction, Beijing, China, Nov. 20-24, 2011, 5-8.
- [2]. Ye.H. Hayrapetyan, H.S. Petosyan, H.A. Hunanyan, A.S. Tsaturyan, High-precision two-phase laser rangefinder PFSD-1,2 international scientific conference on construction the formation of living environment 2019 (FORM 2019), Tashkent, April 18-21, 2019, 1-9.
- [3]. T.E. Chaddock, Gastric emptying of a nutritionally balanced liquid diet, in: E.E. Daniel (ed.), Proceedings of the Fourth International Symposium on Gastrointestinal Motility, ISGM4, 4-8 September 1973, Seattle, WA, Mitchell Press, Vancouver, British Columbia, Canada, 1974, 83-92.
- [4]. N. Yasuda, S.-i. Takagi, A. Toriumi, Spectral shape analysis of infrared absorption of thermally grown silicon dioxide films, in: T. Hattori, K. Wada, A. Hiraki (eds.), Proceedings of the Second International Symposium on the Control of Semiconductor Interfaces, ISCSI-2, Karuizawa, Japan, October 28-November 1, 1997, Appl. Surf. Sci. 117-118 (June (II), 1997, 216-220.
- [5]. M.M. Badalyan, A.K. Karapetyan, L.M. Ter-Oganesyan, Vovlechenie otkhodov nerudnoy promyshlennosti v proizvodstvo stroitel'nykh materialov i izdeliy. Krizisnoe upravlenie i tekhnologii. Mezhdunarodnaya konferentsiya, Nov. 12-13, 2 (15), 2019, 179-185.

Patent

- [1]. K.S. Gunashyan, E.A. Hayrapetyan, V.G. Harytunyan, Kh.V. Vardanyan, Microwave modulator-light demodulator, RR patent 1420367 (1988).
- [2]. K.S. Gyunashyan, E.A. Hayrapetyan, Phase light range finder, RR Patent 1598613 (1990).

Information about author/s (in separate file)

Information about author/s - **name, academic degree, rank**, affiliation, position held, e-mail address should be given.

ADDRESS : Str.Teryan 105, Yerevan



: (+37410) 54 74 12

URL : <https://www.jaer.nuaca.am/>

